

## Occurrence of Hyperon Superfluidity in Neutron Star Cores \*

Tatsuyuki TAKATSUKA,<sup>1</sup> Shigeru NISHIZAKI,<sup>1</sup>  
Yasuo YAMAMOTO<sup>2</sup> and Ryozo TAMAGAKI<sup>3</sup>

<sup>1</sup>*Faculty of Humanities and Social Sciences, Iwate University,  
Morioka 020-8550, Japan*

<sup>2</sup>*Physics Section, Tsuru University, Tsuru 402-8555, Japan*

<sup>3</sup>*Kamitakano Maeda-Cho 26-5, Kyoto 606-0097, Japan*

(Received November 1, 2005)

Superfluidity of  $\Lambda$  and  $\Sigma^-$  admixed in neutron star (NS) cores is investigated realistically for hyperon ( $Y$ )-mixed NS models obtained using a  $G$ -matrix-based effective interaction approach. Numerical results for the equation of state (EOS) with the mixing ratios of the respective components and the hyperon energy gaps including the temperature dependence are presented. These are meant to serve as physical inputs for  $Y$ -cooling calculations of NSs. By paying attention to the uncertainties of the EOS and the  $YY$  interactions, it is shown that both  $\Lambda$  and  $\Sigma^-$  are superfluid as soon as they appear although the magnitude of the critical temperature and the density region where superfluidity exists depend considerably on the  $YY$  pairing potential. Considering momentum triangle condition and the occurrence of superfluidity, it is found that a so-called “hyperon cooling” (neutrino-emission from direct Urca process including  $Y$ ) combined with  $Y$ -superfluidity may be able to account for observations of the colder class of NSs. It is remarked that  $\Lambda$ -hyperons play a decisive role in the hyperon cooling scenario. Some comments are given regarding the consequences of the less attractive  $\Lambda\Lambda$  interaction recently suggested by the “NAGARA event”  ${}^6_{\Lambda\Lambda}\text{He}$ .

### §1. Introduction

Neutron stars (NSs) are primarily composed of neutrons, with a small amount of protons, together with electrons and muons to assure the charge neutrality of the system. With the increase of the total baryon density  $\rho$  toward the central region, however, hyperons ( $Y$ ), such as  $\Lambda$ ,  $\Sigma^-$  and  $\Xi^-$ , begin to appear as new components. This is because the chemical potential of the predominant neutron component gets higher with  $\rho$ , and eventually it becomes energetically economical for the system to replace neutrons at the Fermi surface by  $Y$  through a strangeness non-conserving weak interaction, in spite of the cost of the higher rest-mass energy. The population of  $Y$  increases with increasing  $\rho$  and hyperons, in addition to nucleons, become important constituents of NS cores.

Internal composition and structure strongly affect the thermal evolution of NSs, and this problem has been extensively studied from various points of view.<sup>4)–18)</sup> The participation of  $Y$  provides a much faster cooling mechanism due to the very efficient neutrino-emission processes,<sup>19)</sup> the so-called “hyperon direct Urca” (abbreviated as  $Y$ -DUrca; e.g.,  $\Lambda \rightarrow p + l + \bar{\nu}_l$ ,  $\Sigma^- \rightarrow \Lambda + l + \bar{\nu}_l$  and their inverse processes;  $l \equiv e^-$  or  $\mu^-$ ), compared to the standard cooling mechanism, called the “modified

---

\* A part of this work has been reported in Refs. 1) – 3).

Urca” (MUrca; e.g.,  $n + n \rightarrow n + p + l + \bar{\nu}_l$ ,  $n + p \rightarrow p + p + l + \bar{\nu}_l$  and their inverse processes). The  $\nu$ -emission rate for hyperon cooling (Y-DUrca) is larger by 5-6 orders of magnitude than that for standard cooling (MUrca), because in the latter an additional nucleon has to join in the  $\beta$ -decay process in order to satisfy momentum conservation for the reactions. This rapid hyperon cooling is of particular interest in relation to the surface temperature observations of NSs. That is, recent observations suggest that there are at least two classes of NSs, hotter ones and colder ones, and these findings have motivated studies on cooling scenarios to explain the two classes consistently. Standard cooling, together with a frictional heating mechanism, can explain the hotter ones, but not the colder ones.<sup>10)</sup> Then the fast non-standard hyperon cooling shows up as a candidate to explain the colder ones. The direct action of hyperon cooling, however, leads to a serious problem of “too rapid cooling” incompatible with observations and therefore some suppression mechanism for an enhanced  $\nu$ -emission rate is necessary. The most natural choice as a possible mechanism to play this suppressive role is hyperon superfluidity.

In this paper, we study whether hyperons admixed can be superfluids and show that indeed they can.<sup>1)–3)</sup> This implies that there is strong possibility that the hyperon cooling scenario, combined with the  $Y$ -superfluidity, is the mechanism responsible for fast non-standard cooling compatible with the data of the colder class of NSs. In our preceding works,<sup>20)–22)</sup> we studied the hyperon energy gap  $\Delta_Y$  responsible for  $Y$ -superfluids using a simplified treatment in which the  $\rho$ -dependent  $Y$ -mixing ratios  $y_Y (\equiv \rho_Y/\rho)$  relevant to the Fermi momentum  $q_{FY}$  and the  $\rho$ -dependent effective-mass parameter  $m_Y^*$  are taken as parameters. In the present work, we use  $\rho$ -dependent  $y_Y(\rho)$  and  $m_Y^*(\rho)$  based on the  $Y$ -mixed NS models in order to derive a realistic  $\Delta_Y$  in a  $\rho$ -dependent way. Also, we present profile functions representing the temperature-dependence of  $\Delta_Y$ , which is necessary for treating the thermal evolution of NSs, and attempt to provide the basic physical quantities for cooling calculations of a realistic level.

This paper is organized as follows. In §2, our NS models with  $Y$ -mixing, calculated using a  $G$ -matrix effective interaction approach, are presented, together with the composition, the equation of state (EOS) and the physical quantities necessary for the energy gap calculations. The energy gap equation including a finite-temperature ( $T > 0$ ) case is treated in §3, where some comments are given on the important ingredients in the gap equation, i.e.,  $m_Y^*(\rho)$  and the  $YY$  pairing interactions in comparison with the case of nucleons. Results for  $\Delta_Y$  and the profile functions are given in §4, together with discussion regarding the momentum triangle condition for  $Y$ -DUrca processes and the superfluid suppression of  $\nu$ -emissivities. In addition, in §5, we discuss how a less attractive  $\Lambda\Lambda$  interaction inferred from  ${}^6_{\Lambda\Lambda}\text{He}$  observed recently affects the realization of  $Y$ -superfluidities. The last section, §6, contains a summary and remarks.

## §2. Neutron Star Models with Hyperons

In this section, we calculate the EOS of  $Y$ -mixed NS matter responsible for  $Y$ -mixed NS models and also obtain the  $\rho$ -dependent  $y_Y$  and  $m_Y^*$  of hyperons necessary

for the energy gap calculations. For simplicity, we ignore the mixing of the  $\Xi^-$  component and restrict our investigation to  $Y \equiv \{\Lambda, \Sigma^-\}$  as the hyperon components, since it would be less likely for  $\Xi^-$  to appear due to the larger mass ( $m_{\Xi^-} = 1321$  MeV compared to  $m_{\Lambda} = 1116$  MeV and  $m_{\Sigma^-} = 1192$  MeV). We treat  $Y$ -mixed NS matter composed of  $n, p, \Lambda, \Sigma^-, e^-$  and  $\mu^-$  using a  $G$ -matrix based effective interaction approach, with attention to the choice of  $YN$  and  $YY$  interactions compatible with hypernuclear data:<sup>23)–25)</sup>

1. We construct the effective  $YN$  and  $YY$  local potentials,  $\tilde{V}_{YN}$  and  $\tilde{V}_{YY}$ , in a  $\rho$ - and  $y_Y$ -dependent way, from the  $G$ -matrix calculations performed for  $\{n + Y\}$  matter with a given  $\rho$  and  $y_Y$ . In these calculations, we use the  $YN$  and  $YY$  interactions from the Nijmegen model D hard core potential<sup>26)</sup> (NHC-D) with a slight modification in the  $S$ -state  $\Lambda N$  part (NHC-Dm) as a reasonable choice (details are referred to Ref. 23)). From a view of  $\Lambda$  effective-mass parameter ( $m_{\Lambda}^*$ ) controlling the realization of  $\Lambda$ -superfluidity, which is discussed in the next section, the choice of this NHC-Dm is appropriate since it reproduces  $m_{\Lambda}^* \sim 0.8$  inferred from hypernuclear data.<sup>27)</sup>
2. For the effective  $NN$  local potential  $\tilde{V}_{NN}$ , we use  $\tilde{V}_{RSC}$  supplemented by  $\tilde{V}_{TNI}$ , i.e.,  $\tilde{V}_{NN} = \tilde{V}_{RSC} + \tilde{V}_{TNI}$  where  $\tilde{V}_{RSC}$ <sup>28)</sup> is the effective two-nucleon potential constructed from the  $G$ -matrix calculations in asymmetric nuclear matter with the Reid soft-core potential and  $\tilde{V}_{TNI}$ <sup>29)</sup> is a phenomenological three-nucleon interaction (TNI) of the Lagaris-Pandharipande type.<sup>30),31)</sup> The potential  $\tilde{V}_{TNI}(= \tilde{V}_{TNA} + \tilde{V}_{TNR})$  consists of two parts, the attractive  $\tilde{V}_{TNA}$  and the repulsive  $\tilde{V}_{TNR}$ , and is expressed in the form of a two-body potential with a  $\rho$ -dependence. At high densities the contribution from  $\tilde{V}_{TNA}$  is minor, while that from  $\tilde{V}_{TNR}$  dominates, and TNI brings a strong repulsion with increasing  $\rho$ . The parameters inherent in  $\tilde{V}_{TNI}$  are determined so that  $\tilde{V}_{TNI}$  can reproduce the empirical saturation properties of symmetric nuclear matter (binding energy  $E_B = -16$  MeV and saturation density  $\rho_0 \equiv 0.17$  nucleons/fm<sup>3</sup>) and the nuclear incompressibility  $\kappa$ .
3. On the basis of  $\tilde{V}_{NN}$ ,  $\tilde{V}_{YN}$  and  $\tilde{V}_{YY}$ , we calculate the fractions  $y_i$  for the respective components ( $i = n, p, \Lambda, \Sigma^-, e^-$  and  $\mu^-$ ) in  $\beta$ -equilibrium, under the conditions of charge neutrality, chemical equilibrium and baryon number conservation, and derive the EOS and  $m_Y^*(\rho)$  of  $Y$ -mixed NS matter.

Using the EOS thus obtained, we solve the so-called TOV equation and obtain NS models with a  $Y$ -mixed core. In the calculations, extended use of our  $G$ -matrix-based effective interactions to high-density regime is inevitable, and this introduces uncertainties with increasing  $\rho$ . These uncertainties, however, would not be serious because the  $\rho$ -dependence of  $E$  (the energy per particle), namely the EOS, is similar to that obtained with more realistic treatments, as shown in Fig.1 for the TNI6 case, for example. Our NS models are specified by the parameter  $\kappa$  relevant to  $\tilde{V}_{NN}$ , which is a measure of the stiffness of the nuclear-part EOS ( $N$ -part EOS). We consider three cases;  $\kappa = 250$  MeV (hereafter, referred to as TNI2), 300 MeV (TNI3) and 280 MeV (TNI6). TNI2 is a soft EOS case, TNI3 is a stiffer EOS case and TNI6 is between the two, giving respectively the maximum mass  $M_{\max}$  of NSs sustained by the EOS as

$M_{\max} \simeq 1.62M_{\odot}$ ,  $1.88M_{\odot}$  and  $1.78M_{\odot}$  for normal NSs without  $Y$ -mixing. In Fig.1, we compare our EOSs for neutron matter with those by the Illinois group currently regarded as most realistic. We stress that our EOSs cover almost the entire range from soft to stiff cases allowed by realistic EOSs derived using a more sophisticated many-body approach.<sup>32),33)</sup>

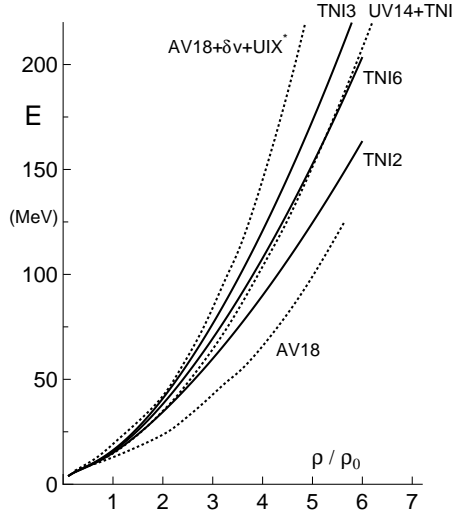


Fig. 1. Energy per particle  $E$  versus density  $\rho$ , corresponding to the EOS of neutron matter ( $\rho_0 = 0.17$  nucleons/ $\text{fm}^3$  being the nuclear density). The solid curves labeled TNI2, TNI6 and TNI3 are respectively soft, intermediate and the stiff EOSs considered here. The EOSs from the Illinois group, i.e., AV18<sup>33)</sup> (softest), UV14+TNI<sup>32)</sup> (intermediate) and AV18+ $\delta v$ +UIX<sup>33)</sup> (stiffest), are also displayed by the dotted lines. It is seen that our EOSs are well within the range from the softest to stiffest EOSs currently taken as realistic.

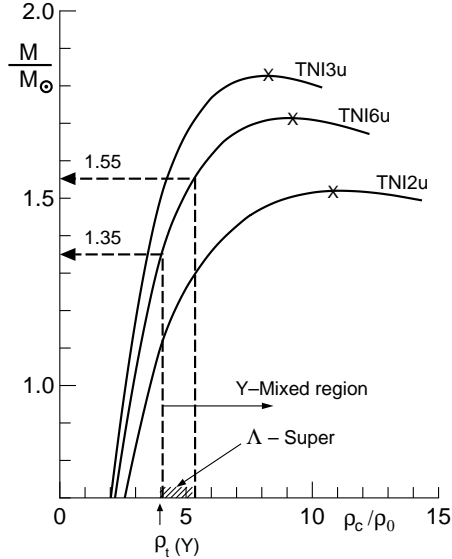


Fig. 2. Mass  $M$  versus central density  $\rho_c$  for neutron stars (NSs) corresponding to the EOS of hyperon ( $Y$ )-mixed neutron star matter (TNI2u, TNI6u and TNI3u), where repulsion from the three-nucleon interaction (TNI) is introduced universally (see the main text for details). The crosses denote the maximum mass points. The threshold density  $\rho_t(Y)$  of  $Y$ -mixing and the density region, in which there exists  $\Lambda$ -superfluid for ND-Soft pairing interaction, are also shown in order to indicate the  $M$  and EOS dependences of the  $\Lambda$ -superfluid phase.

Table I. Profile (mass  $M_{\max}$ , radius  $R$  and central density  $\rho_c$ ) of the maximum-mass NSs depicted in Fig.2 for EOSs from soft (TNI2u) to stiff (TNI3u). The threshold density  $\rho_t(Y)$  indicating the portion of  $Y$ -mixed core is also listed for the  $\Lambda$  and  $\Sigma^-$  cases.

EOS	$\rho_t(\Lambda)/\rho_0$	$\rho_t(\Sigma^-)/\rho_0$	$M_{\max}/M_{\odot}$	$R/\text{km}$	$\rho_c/\rho_0$
TNI2u	4.01	4.06	1.52	8.43	11.08
TNI6u	4.02	4.06	1.71	9.16	9.07
TNI3u	4.01	4.01	1.83	9.55	8.26

Table II. (a) EOS of  $Y$ -mixed NS matter with mixing ratio  $y_i$  of the constituents ( $i = n, p, \Lambda, \Sigma^-, e^-, \mu^-$ ) for the case of TNI2u. The energy density  $e$  is in units of  $\text{MeV}/\text{fm}^3$  and the pressure  $P$  is in units of  $\text{dyn}/\text{cm}^2$ .

$\rho/\rho_0$	$y_n$	$y_p$	$y_\Lambda$	$y_{\Sigma^-}$	$y_{e^-}$	$y_{\mu^-}$	$e$	$P$
0.5	0.9684	0.0316	0.	0.	0.0316	0.	80.5	5.51E+32
1.0	0.9499	0.0501	0.	0.	0.0451	0.0050	161.9	3.67E+33
1.5	0.9409	0.0591	0.	0.	0.0464	0.0128	244.9	1.13E+34
2.0	0.9380	0.0620	0.	0.	0.0453	0.0168	330.1	2.40E+34
2.5	0.9371	0.0629	0.	0.	0.0439	0.0191	417.6	4.23E+34
3.0	0.9368	0.0632	0.	0.	0.0426	0.0206	507.7	6.70E+34
3.5	0.9368	0.0632	0.	0.	0.0415	0.0216	600.9	9.92E+34
4.0	0.9371	0.0629	0.	0.	0.0406	0.0224	697.2	1.40E+35
4.5	0.8561	0.0862	0.0262	0.0315	0.0354	0.0193	796.8	1.80E+35
5.0	0.7633	0.1127	0.0574	0.0667	0.0301	0.0159	899.2	2.25E+35
5.5	0.6824	0.1354	0.0859	0.0963	0.0258	0.0133	1004.8	2.78E+35
6.0	0.6135	0.1545	0.1109	0.1211	0.0223	0.0111	1113.5	3.38E+35
6.5	0.5556	0.1701	0.1327	0.1416	0.0193	0.0092	1225.6	4.08E+35
7.0	0.5071	0.1827	0.1518	0.1584	0.0167	0.0076	1341.3	4.87E+35
7.5	0.4660	0.1929	0.1687	0.1723	0.0144	0.0062	1460.7	5.77E+35
8.0	0.4308	0.2013	0.1838	0.1840	0.0123	0.0049	1584.1	6.77E+35
9.0	0.3734	0.2143	0.2096	0.2027	0.0088	0.0028	1843.3	9.10E+35
10.0	0.3277	0.2243	0.2309	0.2170	0.0060	0.0013	2120.3	1.19E+36
11.0	0.2898	0.2329	0.2485	0.2288	0.0038	0.0003	2416.3	1.52E+36
12.0	0.2570	0.2410	0.2631	0.2388	0.0022	0.0000	2732.5	1.90E+36
13.0	0.2272	0.2492	0.2754	0.2481	0.0011	0.0000	3069.9	2.34E+36
14.0	0.1983	0.2581	0.2859	0.2577	0.0004	0.0000	3429.3	2.82E+36
15.0	0.1675	0.2689	0.2948	0.2688	0.0001	0.0000	3811.6	3.36E+36

(b) Same as (a), but for the TNI6u case.

$\rho/\rho_0$	$y_n$	$y_p$	$y_\Lambda$	$y_{\Sigma^-}$	$y_{e^-}$	$y_{\mu^-}$	$e$	$P$
0.5	0.9682	0.0318	0.	0.	0.0318	0.	80.5	5.87E+32
1.0	0.9473	0.0527	0.	0.	0.0468	0.0058	162.0	4.00E+33
1.5	0.9369	0.0631	0.	0.	0.0488	0.0143	245.4	1.31E+34
2.0	0.9341	0.0659	0.	0.	0.0475	0.0184	331.2	2.91E+34
2.5	0.9341	0.0659	0.	0.	0.0455	0.0203	420.2	5.26E+34
3.0	0.9349	0.0651	0.	0.	0.0437	0.0214	512.6	8.47E+34
3.5	0.9358	0.0643	0.	0.	0.0421	0.0221	608.8	1.27E+35
4.0	0.9366	0.0634	0.	0.	0.0408	0.0226	709.2	1.80E+35
4.5	0.8550	0.0869	0.0261	0.0321	0.0354	0.0193	814.0	2.37E+35
5.0	0.7609	0.1136	0.0578	0.0677	0.0300	0.0159	923.0	3.02E+35
5.5	0.6797	0.1363	0.0865	0.0975	0.0257	0.0132	1036.4	3.79E+35
6.0	0.6110	0.1553	0.1116	0.1222	0.0221	0.0109	1154.5	4.68E+35
6.5	0.5534	0.1707	0.1334	0.1425	0.0191	0.0091	1277.6	5.71E+35
7.0	0.5052	0.1831	0.1525	0.1591	0.0165	0.0075	1406.1	6.89E+35
7.5	0.4645	0.1932	0.1694	0.1729	0.0142	0.0061	1540.1	8.23E+35
8.0	0.4296	0.2015	0.1845	0.1845	0.0122	0.0048	1680.0	9.73E+35
9.0	0.3725	0.2144	0.2102	0.2029	0.0087	0.0028	1978.6	1.32E+36
10.0	0.3271	0.2244	0.2313	0.2172	0.0059	0.0013	2304.1	1.75E+36
11.0	0.2893	0.2330	0.2489	0.2289	0.0038	0.0003	2658.3	2.25E+36
12.0	0.2566	0.2411	0.2635	0.2389	0.0022	0.0000	3043.3	2.83E+36

(c) Same as (a), but for the TNI3u case.

$\rho/\rho_0$	$y_n$	$y_p$	$y_\Lambda$	$y_{\Sigma^-}$	$y_{e^-}$	$y_{\mu^-}$	$e$	$P$
0.5	0.9681	0.0319	0.	0.	0.0319	0.	80.5	6.17E+32
1.0	0.9454	0.0546	0.	0.	0.0481	0.0065	162.1	4.21E+33
1.5	0.9334	0.0666	0.	0.	0.0509	0.0158	245.6	1.42E+34
2.0	0.9302	0.0698	0.	0.	0.0498	0.0201	332.0	3.26E+34
2.5	0.9306	0.0694	0.	0.	0.0475	0.0219	422.0	6.01E+34
3.0	0.9321	0.0679	0.	0.	0.0452	0.0226	516.0	9.80E+34
3.5	0.9339	0.0661	0.	0.	0.0432	0.0230	614.5	1.48E+35
4.0	0.9354	0.0646	0.	0.	0.0415	0.0231	718.1	2.11E+35
4.5	0.8457	0.0907	0.0274	0.0362	0.0353	0.0192	826.8	2.79E+35
5.0	0.7516	0.1172	0.0594	0.0718	0.0297	0.0157	940.6	3.59E+35
5.5	0.6712	0.1395	0.0881	0.1012	0.0254	0.0129	1059.8	4.54E+35
6.0	0.6038	0.1578	0.1132	0.1253	0.0218	0.0107	1184.9	5.65E+35
6.5	0.5475	0.1726	0.1349	0.1449	0.0189	0.0089	1316.2	6.94E+35
7.0	0.5004	0.1846	0.1539	0.1611	0.0163	0.0073	1454.2	8.41E+35
7.5	0.4605	0.1943	0.1707	0.1744	0.0140	0.0059	1599.1	1.01E+36
8.0	0.4263	0.2023	0.1857	0.1857	0.0120	0.0047	1751.3	1.19E+36
9.0	0.3702	0.2148	0.2113	0.2037	0.0085	0.0027	2079.3	1.63E+36
10.0	0.3255	0.2246	0.2322	0.2177	0.0058	0.0012	2440.9	2.17E+36

As a peculiar property of the  $Y$ -mixed NS models, we remark that the  $Y$ -mixing causes a dramatic softening effect on the EOS and consequently  $M_{\max}$  for  $Y$ -mixed NSs is greatly reduced.<sup>23)–25)</sup> For example,  $M_{\max} \simeq 1.62M_\odot$  for the case without  $Y$  is reduced to  $M \simeq 1.08M_\odot$  for the case with  $Y$ , contradicting the condition that  $M_{\max}$  should be larger than  $M_{\text{obs}}$  (PSR1913+16)= $1.44M_\odot$ , the observed NS mass for PSR1913+16. This inconsistency between theory and observation cannot be resolved by using a stronger  $NN$  repulsion, as seen from  $M_{\max} \simeq 1.08M_\odot \rightarrow 1.09M_\odot \rightarrow 1.10M_\odot$  for TNI2 $\rightarrow$ TNI6 $\rightarrow$ TNI3 with increasing  $\kappa$ . This is because as the  $N$ -part EOS becomes stiffer, the  $Y$ -mixed phase develops from lower densities, and as a result, the softening effect becomes stronger, making the enhanced  $NN$  repulsion ineffective. The problem that the relation  $M_{\max} < M_{\text{obs}}$  is predicted for  $Y$ -mixed NSs is also seen in other approaches,<sup>34),35)</sup> and it is encountered in an almost model-independent way, which interestingly suggests that some “extra repulsion” must exist in hypernuclear systems, namely,  $YN$  and  $YY$  interaction parts. As one possible such repulsion, we try to introduce a repulsion from the three-body force  $\tilde{V}_{\text{TNR}}$  in TNI also into the  $YN$  and  $YY$  parts, as well as the  $NN$  part (hereafter called the “universal inclusion of TNI” and denoted simply by TNIu),<sup>23)–25)</sup> because the importance of the three-body interaction is well recognized for nuclear systems and should not be restricted to nuclear systems ( $NN$  part). When this is done, we have a moderate softening, not a dramatic one, as before, and we obtain a larger  $M_{\max}$  that satisfies the condition  $M_{\max} > 1.44M_\odot$ ;  $M_{\max} \simeq 1.52M_\odot$ ,  $1.71M_\odot$  and  $1.83M_\odot$  for TNI2u, TNI6u and TNI3u, respectively. We also note that the realization of a  $Y$ -mixed phase is pushed to the higher density side; the threshold density  $\rho_t(Y) \simeq (2.5 - 3)\rho_0$  for no extra repulsion whereas  $\rho_t(Y) \simeq 4\rho_0$  for the universal inclusion of the three-body repulsion. These results suggest that  $\rho_t(Y)$  is not so low as currently believed ( $\rho_t(Y) \sim 2\rho_0$ ) but rather high ( $\sim 4\rho_0$ ), as far as consistency between the  $Y$ -mixed

EOS and the NS mass observed is taken into account.<sup>25)</sup> In our calculations, the threshold densities for the appearance of  $\Lambda$  and  $\Sigma^-$  are almost the same ( $\rho_t(\Lambda) \simeq \rho_t(\Sigma^-) \simeq 4\rho_0$ ), in contrast to the relation  $\rho_t(\Sigma^-) < \rho_t(\Lambda)$  currently thought to hold. This comes from the fact that the repulsive nature of  $\Sigma^-n$  interaction suggested by hypernuclear data is duly taken into account (i.e., by using the NHC-D potential). Otherwise, we have  $\rho_t(\Sigma^-) < \rho_t(\Lambda)$ ; the weakening of the  $\Sigma^-n$  repulsion as  $\tilde{V}_{\Sigma^-n} \rightarrow \tilde{V}_{\Sigma^-n}/3$ , for example, leads to  $\rho_t(\Sigma^-) \simeq 3\rho_0$  and  $\rho_t(\Lambda) \simeq 4.1\rho_0$ . In Table I, we list the parameter profiling the  $Y$ -mixed NSs that correspond to the maximum mass  $M_{\max}$  and illustrate in Fig.2 the  $M$ - $\rho_c$  relationships indicating how the  $Y$ -mixed core region depends on  $M$  and the EOS. We list in Table II the numerical values of the composition and EOS for  $Y$ -mixed NSs.

### §3. Energy gap equation for hyperon pairing

As shown in the preceding section, hyperons participate at high densities ( $\rho \gtrsim \rho_t(Y) \sim 4\rho_0$ ), but the fractional density  $\rho_Y (= y_Y \rho)$  is relatively low due to small contamination, e.g.,  $y_Y \lesssim 0.1$  for the density region  $\rho \simeq (\rho_t(Y) \sim 6\rho_0)$  of interest. Here, we limit our study to the treatment of hyperon pairing in a non-relativistic framework. We do this both because the fractional density of hyperons is not high and also because, in its present form, the treatment<sup>36)</sup> in the relativistic framework involves ambiguities coming from the introduction of a phenomenological cutoff mass in the pairing interaction. Corresponding to the small  $\rho_Y$ , the scattering energy  $E_{YY}^{\text{lab}}$  in the laboratory frame for a  $(\vec{q}, -\vec{q})$ -Cooper pair near the Fermi surface ( $q \simeq q_{FY} = (3\pi^2\rho_Y)^{1/3}$  with  $q_{FY}$  being the Fermi momentum of  $Y$ ) is at most 110 MeV, estimated by  $E_{YY}^{\text{lab}} = 4E_{FY} = 4\hbar^2 q_{FY}^2 / 2M_Y$  with  $E_{FY}$  and  $M_Y$  being the Fermi kinetic energy and the mass of hyperons, respectively. This means that the pairing interaction  $V_{YY}$  responsible for  $Y$ -superfluidity should be that in the  $^1S_0$  pair state ( $V_{YY}(^1S_0)$ ) which is most attractive at low scattering energies. Thus the gap equation to be treated here is of the well-known  $^1S_0$ -type:

$$\Delta_Y(q) = -\frac{1}{\pi} \int_0^\infty q'^2 dq' \langle q' | V_{YY}(^1S_0) | q \rangle \frac{\Delta_Y(q')}{E_Y(q')} \tanh\left(\frac{E_Y(q)}{2\kappa_B T}\right), \quad (3.1)$$

$$E_Y(q') \equiv \sqrt{\tilde{\epsilon}_Y^2(q') + \Delta_Y^2(q')}, \quad (3.2)$$

$$\tilde{\epsilon}_Y(q') \equiv \epsilon_Y(q') - \epsilon_Y(q_{FY}) \simeq \frac{\hbar^2}{2M_Y^*} (q'^2 - q_{FY}^2), \quad (3.3)$$

$$\langle q' | V_{YY}(^1S_0) | q \rangle \equiv \int_0^\infty r^2 dr j_0(q'r) V_{YY}(r; ^1S_0) j_0(qr), \quad (3.4)$$

including the case of finite temperature with  $\kappa_B$  being the Boltzman constant. In the above expressions,  $\Delta_Y(q)$  is the energy gap function,  $\epsilon_Y(q)$  the single-particle energy and  $M_Y^*$  the effective mass of  $Y$ . For simplicity, the effective mass approximation for  $\epsilon_Y(q)$  is adopted in Eq.(3.3). We use a bare  $V_{YY}(^1S_0)$  for the pairing interaction and do not introduce the  $G$ -matrix based effective interaction  $\tilde{V}_{YY}(^1S_0)$  in place

of  $V_{YY}(^1S_0)$  as done by Balberg and Barnea,<sup>37)</sup> because the gap equation plays the dual roles of taking account of the pairing correlation and the short-range correlation (s.r.c.) simultaneously and hence use of  $\tilde{V}_{YY}(^1S_0)$  leads to incorrect results with larger energy gaps due to the double counting of s.r.c..

The gap equation (Eq.(3.1)) is solved numerically with  $q_{FY}$ ,  $M_Y^*$  and  $V_{YY}(^1S_0)$  given. We solve it exactly without any approximation, using an iterative technique. The  $q_{FY}$  (equivalently  $y_Y$ ) and  $M_Y^*$  (equivalently the effective mass parameter  $m_Y^* \equiv M_Y^*/M_Y$ ) are derived in §2. In the following, we make some comments regarding the important ingredients in Eq.(3.1),  $m_Y^*$  and  $V_{YY}(^1S_0)$ , controlling the resulting energy gap  $\Delta_Y \equiv \Delta_Y(q_{FY})$ .

i) Effective mass parameter  $m_Y^*$

Generally, the energy gap is very sensitive to  $m_Y^*$  and a larger value is obtained for larger  $m_Y^*$ . This is due to the fact that the energy cost for the excitation of a  $YY$ -pair ( $\tilde{\epsilon}_Y(q)$  in Eq.(3.3)) is smaller for larger  $M_Y^*$  ( $\equiv m_Y^*M_Y$ ). In this sense,  $Y$ -superfluidity is more likely to occur than superfluidity of nucleons, since  $m_Y^* \simeq (0.8 \sim 1.2)$  is significantly larger than  $m_N^* \simeq (0.5 \sim 0.7)$  for  $\rho \gtrsim 4\rho_0$  as shown in Fig.3. Moreover, the fact that  $M_Y \simeq (1116 \text{ MeV or } 1192 \text{ MeV}) > M_N \simeq 940 \text{ MeV}$  strengthens this tendency. Since the single-particle energy has the same effect when  $M_Y^* = M_N^*$ , the effect of  $m_Y^* = 0.8$  in the  $YY$  pairing corresponds to that of  $m_N^* = (M_Y/M_N)m_Y^* \simeq 1.0$  in the  $NN$  pairing, for the  $Y \equiv \Sigma^-$  case. A comparison of the  $\Lambda$  and  $\Sigma^-$  cases reveals that  $\Sigma^-$ -superfluidity is more favourable than  $\Lambda$ -superfluidity since  $m_{\Sigma^-}^* > m_{\Lambda}^*$  and in addition  $M_{\Sigma^-} > M_{\Lambda}$ . That is, the resulting energy gaps for baryon superfluids satisfy the relation  $\Delta_{\Sigma^-} > \Delta_{\Lambda} > \Delta_N$ , as far as the role of effective mass is concerned.

ii) Pairing potential

The attractive effect of the  $YY$  pairing potential  $V_{YY}(^1S_0)$  is a main agency for the occurrence of  $Y$ -superfluidity. Our present knowledge of  $V_{YY}(^1S_0)$ , however, is very limited. As in previous works, we adopt three potentials, the ND-Soft<sup>2),21),38)</sup> \*\*, Ehime<sup>39)</sup> and FG-A,<sup>40)</sup> with due regard to the present uncertainties of the  $YY$  potentials. They are commonly based on the one-boson-exchange (OBE) hypothesis with  $SU(3)$  symmetry in the framework of nonet mesons and octet baryons ( $B$ ). The main differences among them regard the treatments of the short-range interactions and the kinds of mesons introduced. The ND-Soft potential is a soft-core version of the original Nijmegen hard-core model D (NHC-D)<sup>26)</sup> obtained as a superposition of three-range Gaussian functions and is constructed so as to fit the  $t$ -matrix from NHC-D with the hard-core radii being taken as 0.5 fm. The soft-core version is used for the sake of convenience in the treatment of the gap equation. The Ehime potential is characterized by an application of the OBE scheme throughout all interaction ranges and by the addition of a phenomenological neutral scalar meson to take the  $2\pi$ -correlation effects of this sort into account. It consists of a superposition of Yukawa-type functions in  $r$ -space regularized by the form factors in momentum space and has velocity-dependent terms. The FG-A potential is based on the OBE-

---

\*\* In the Table I of Ref. 2),  $V_{i\Sigma^-}^c$  with  $i = 2$  should be corrected as  $-2.9232 \rightarrow -29.232$ .



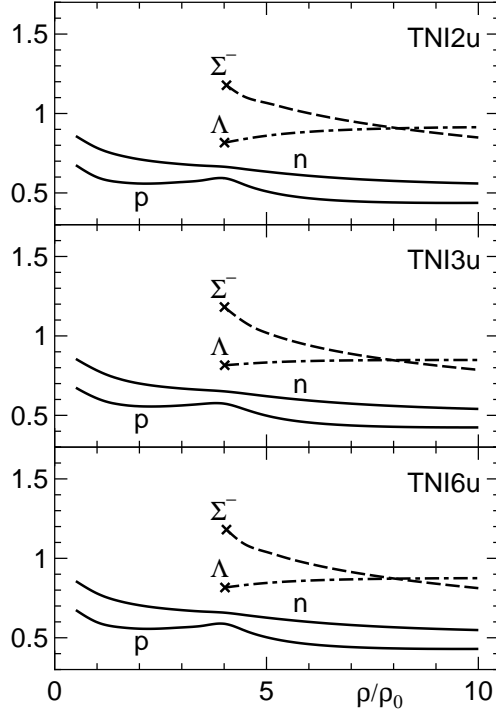


Fig. 3. Effective mass parameters  $m_i^*$  for baryon components ( $i = n, p, \Lambda, \Sigma^-$ ) as functions of  $\rho$  in the three cases TNI2u, TNI6u and TNI3u for  $Y$ -mixed NS matter with different stiffnesses. The crosses denote the threshold points for the  $Y$ -mixing.

scheme, in which the  $\sigma$ -meson is treated in the nonet scheme by taking account of the broad width of  $\sigma$ - and  $\rho$ -mesons, and it has a Gaussian soft-core repulsion with strengths constrained by the  $SU(3)$  representation of two baryons. This potential includes the velocity-dependence and the retardation effects.

Here we add a comment on the treatment of the channel coupling effect (CCE) of  $\Lambda\Lambda$ - $\Sigma\Sigma$ - $\Xi N$  type in these potentials. The ND-Soft is constructed so as to simulate the  $t$ -matrices calculated with the NHC-D in the  $\Lambda\Lambda$  and  $\Xi N$  channels. For simplicity, here, we use only the  $\Lambda\Lambda$ - $\Lambda\Lambda$  diagonal part of ND-Soft, because the  $\Lambda\Lambda$ - $\Xi N$  coupling effect was found to be small for the coupling constant of the model D.\*\*\* In the Ehime case, CCE is irrelevant, because it is constructed in a single-channel approximation. In the FG-A case, however, CCE is significant, and it is taken into account by adding an extra term  $\Delta V_{\text{sim}}(r)$  to the direct-channel part  $V_{\Lambda\Lambda}^D(^1S_0)$ , so that  $V_{\Lambda\Lambda}^{(\text{eff})}(^1S_0) \equiv V_{\Lambda\Lambda}^D(^1S_0) + \Delta V_{\text{sim}}(r)$  simulates the  $^1S_0$   $\Lambda\Lambda$  phase shifts including CCE. In practice, we use this  $V_{\Lambda\Lambda}^{(\text{eff})}(^1S_0)$  as  $V_{\Lambda\Lambda}(^1S_0)$  for the FG-A potential by setting  $\Delta V_{\text{sim}}(r) = 93e^{-(r/r_1)^2} - 1000e^{-(r/r_2)^2}$  MeV with  $r_1 = 1.0$  fm and  $r_2 = 0.6$  fm.

\*\*\* The statement “this channel coupling effect, although small, is included similarly through the original  $t$ -matrix to be fitted” appears in Ref. 22) (also similar statements in Refs. 2) and 3)) is inaccurate and should be revised as above.

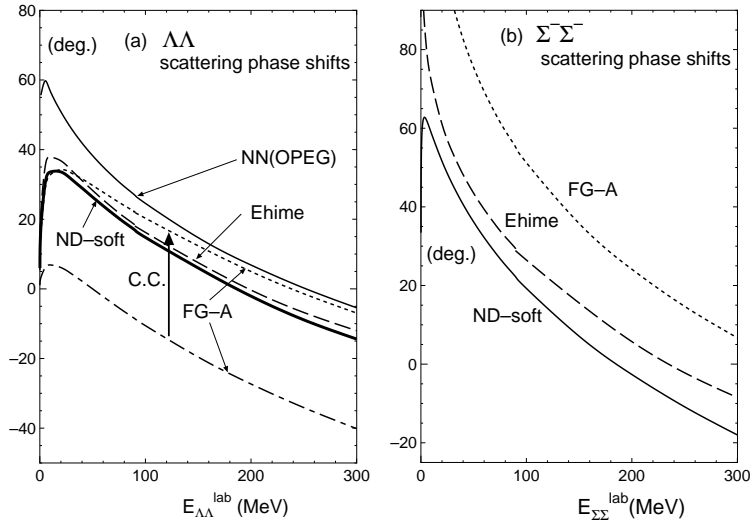


Fig. 4. (a)  $\Lambda\Lambda$  scattering phase shifts in degrees as functions of the laboratory frame energy  $E_{\Lambda\Lambda}^{\text{lab}}$  in MeV for three  $\Lambda\Lambda$   $^1S_0$  potentials (ND-Soft, Ehime and FG-A) explained in the text.  $NN$  scattering phase shifts from the OPEG-1E potential are also shown for comparison. The  $\Lambda\Lambda$ - $\Sigma\Sigma$ - $\Xi N$  channel coupling (CC) effects are indicated by the arrow for the FG-A case (The long dash-dotted line is for no CC.). (b) Same as (a), but for  $\Sigma^-\Sigma^-$  scattering.

In Fig.4, the phase shifts from the three potentials are displayed as functions of  $E_{YY}^{\text{lab}}$ . For  $\Lambda\Lambda$ , they give similar results at low  $E_{YY}^{\text{lab}}$ , while the discrepancies among them increase as  $E_{YY}^{\text{lab}}$  increases, which reflects the short-range behavior in the  $YY$  potentials. For the  $YY$  potentials, experimental information exists only for the  $\Lambda\Lambda$  case, i.e., double  $\Lambda$  hypernuclei. It has been confirmed that ND-soft and Ehime reproduce the bond energy  $\Delta B_{\Lambda\Lambda} (\simeq (4 - 5) \text{ MeV})$  for  ${}_{\Lambda\Lambda}^{10}\text{Be}$  and  ${}_{\Lambda\Lambda}^{13}\text{B}$ .<sup>41)–45)</sup> This reproduction is well expected for FG-A because the phase shifts from FG-A are similar to those from ND-Soft and Ehime at low scattering energies. Recently, however, there arises the problem that  $\Delta B_{\Lambda\Lambda} \simeq (4 - 5) \text{ MeV}$  extracted from  ${}_{\Lambda\Lambda}^{10}\text{Be}$  and  ${}_{\Lambda\Lambda}^{13}\text{B}$  (old data) might be too large and instead  $\Delta B_{\Lambda\Lambda} \sim 1 \text{ MeV}$  from  ${}_{\Lambda\Lambda}^6\text{He}$  (the ‘‘NAGARA event’’,<sup>46)</sup> new data) seems to be correct. This suggests that the  $\Lambda\Lambda$  interaction is less attractive than previously thought. If this is true, it has a significant implication for the realization of  $Y$ -superfluidity. Discussion of this problem is given in §5.

## §4. Numerical results and discussion

### 4.1. Realization of hyperon superfluidity

We discuss how the energy gap for hyperon pairing can be realized by referring to the well-known case of nucleon pairing. We focus on the effects of pairing interactions and effective-mass parameters. For this purpose, the energy gaps  $\Delta_i (\equiv \Delta_i(q_{Fi})$ ;  $i = \Lambda$  and  $p$ ) calculated from Eqs.(3.1)–(3.4) at  $T = 0$ , as functions of the fractional density  $\rho_i (\equiv y_i \rho)$ , are compared in Fig.5, where the pairing interaction  $V_{ii}(^1S_0)$

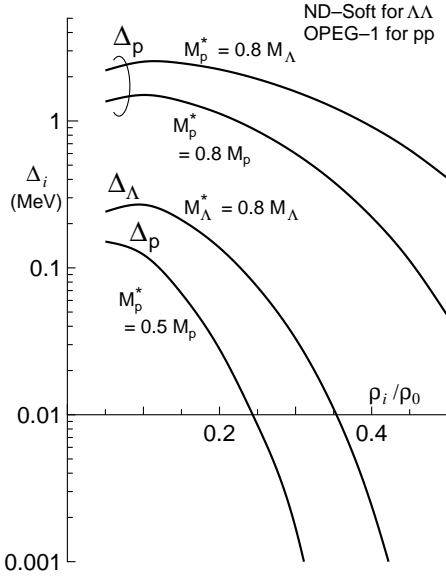


Fig. 5. Energy gaps  $\Delta_i$  for the proton ( $i = p$ ) and Lambda ( $i = \Lambda$ ) as functions of the fractional density  $\rho_i (= y_i \rho)$ . This shows the effects of three factors, i.e., the pairing interaction, effective mass  $M_i^*$  and fractional density  $\rho_i (= y_i \rho)$  controlling the solutions of the energy gap equation. This plot provides an understanding of the realization of  $\Lambda$ -superfluidity. The pairing potential used for  $\Lambda\Lambda$  ( $pp$ ) pairing is ND-Soft (OPEG <sup>1</sup>E-1).

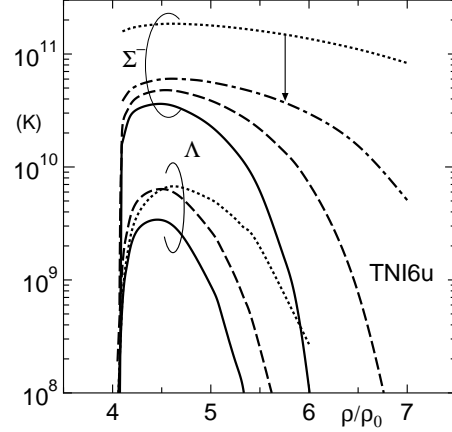


Fig. 6. Hyperon energy gap  $\Delta_i$  ( $i = \Lambda, \Sigma^-$ ) in  $Y$ -mixed NS matter, expressed in terms of the critical temperature  $T_{c_i}^* \simeq 0.57 \Delta_i / \kappa_B$  in Eq.(4.1), as functions of the total baryon density  $\rho$ . The solid, dashed and dotted lines correspond to the ND-Soft, Ehime and FG-A potentials, respectively. The arrow indicates the reduction of  $T_{c_{\Sigma^-}}$  when  $\Lambda\Lambda$  interaction is made less attractive, as suggested by the ‘‘NAGARA event’’  ${}^6_{\Lambda\Lambda}\text{He}$ , by appropriately altering the baryon-baryon interaction model with OBE and SU(3) symmetry frameworks. The reduction of  $\Delta_\Lambda$  is significant and the resulting  $\Delta_\Lambda$  is too small to be determined, i.e.,  $T_{c_\Lambda}^* \ll 10^8$  K.

is taken from the ND-Soft potential for  $i = \Lambda$  and the OPEG <sup>1</sup>E-1 potential<sup>47)</sup> for  $i = p$ . We observe the following three points. First, the relation that  $\Delta_p$  is larger for  $M_p^* = 0.8M_\Lambda$  than for  $M_p^* = 0.8M_p$  means that  $p$ -superfluidity is more likely if the bare mass of  $p$  is as large as that of  $\Lambda$ . Conversely,  $\Lambda$ -superfluidity is realized more easily than  $p$ -superfluidity due to  $M_\Lambda > M_p$  for the same  $m_i^*$ ,  $y_i$  and  $V_{ii}(^1S_0)$ , as mentioned in §3. Second, comparison of  $\Delta_p$  with  $\Delta_\Lambda$  for the same effective-mass ( $M_p^* = M_\Lambda^* = 0.8M_\Lambda$ ) and the same  $y_i$  shows that the influence of the pairing interaction is to make  $p$ -superfluidity more likely than  $\Lambda$ -superfluidity, which is reflected by a stronger attraction of  $V_{NN}(^1S_0)$ , as shown in Fig. 4(a). Third, for the same  $y_i$ , the value of  $\Delta_p$  with  $M_p^* = 0.5M_p$  is smaller than that of  $\Delta_\Lambda$  with  $M_\Lambda^* = 0.8M_\Lambda$ , in spite of the stronger attraction of  $V_{pp}(^1S_0)$ . This suggests that if the actual  $m_i^*(\rho)$  in medium (Fig.3) is taken account (i.e., the case  $m_\Lambda^* > 0.8$  is compared to the case  $m_p^* \sim 0.5$  for  $\rho \gtrsim 4\rho_0$ ),  $\Delta_\Lambda$  would be much larger than  $\Delta_p$ . In fact, as shown just below, we have  $\Lambda$ -superfluidity and also  $\Sigma^-$ -superfluidity in NS cores, but we have no  $p$ -superfluidity due to a significant effect coming from the very small  $m_p^*(\rho)$  and relatively large  $\rho_p$  (namely  $y_p$ ). Thus, we can say that  $Y$ -superfluidity in

dense NS cores occurs as a result of the fact that the attractive effect of  $V_{YY}(^1S_0)$  is not so different from that of  $V_{NN}(^1S_0)$  and is mainly due to the strong influence of  $m_Y^*(\rho)$  which is much larger than  $m_N^*(\rho)$ .

Results for a realistic case with  $\rho$ -dependent  $m_Y^*$  and  $y_Y$  are displayed in Fig.6 for the TNI6u NS model as an example, in terms of the critical temperature  $T_{cY}^*$  for  $Y$ -superfluidity defined by the well-known formula from the near-Fermi-surface approximation,

$$T_{cY}^* \equiv 0.57\Delta_Y/\kappa_B \simeq 0.66\Delta_Y \times 10^{10}K, \quad (4.1)$$

with  $\Delta_Y$  in MeV calculated at  $T = 0$  ( $\Delta_Y \equiv \Delta_Y(q_F, T = 0)$ ). The solid, dashed and dotted lines correspond to  $Y_{YY}(^1S_0)$  from the ND-Soft, the Ehime and the FG-A potentials, respectively. The  $Y$ -superfluidity occurs when  $T_{cY}$  exceeds  $T_{in} \simeq 10^8$  K, the internal temperature of usual middle-aged NSs. The following points are noted:

Table III. Energy gaps  $\Delta_Y$  of  $\Lambda$  and  $\Sigma^-$  in TNI6u  $Y$ -mixed NS matter at zero temperature ( $E = 0$ ) for several densities  $\rho$  and for three  $YY$  pairing interactions; ND-Soft, Ehime and FG-A. The mixing ratios  $y_Y$  and the effective mass parameters  $m_Y^*$  ( $\equiv M_Y^*/M_Y$ ) of hyperons in medium are also given.  $\Delta_Y$  at finite temperature ( $T > 0$ ) is obtained from the profile function  $P(\tau)$  given in §4.2.

$Y$	$\rho/\rho_0$	$y_Y$	$m_Y^*$	$\Delta_Y$ in MeV		
				ND-Soft	Ehime	FG-A
$\Lambda$	4.05	0.00057	0.818	0.006	0.019	0.006
	4.10	0.00225	0.820	0.061	0.133	0.067
	4.15	0.0046	0.821	0.140	0.274	0.168
	4.25	0.0102	0.825	0.274	0.496	0.370
	4.50	0.0261	0.832	0.339	0.638	0.635
	4.75	0.0422	0.839	0.219	0.486	0.641
	5.00	0.0578	0.845	0.089	0.271	0.516
	5.10	0.0638	0.847	0.053	0.196	0.450
	5.25	0.0726	0.850	0.019	0.106	0.348
	5.35	0.0782	0.852	0.008	0.065	0.285
	5.50	0.0865	0.854	0.001	0.025	0.195
6.00	0.1116	0.860	0.	0.	0.027	
$\Sigma^-$	4.10	0.00156	1.165	1.656	2.295	15.866
	4.15	0.0047	1.146	2.428	3.166	16.502
	4.25	0.0123	1.121	3.238	4.125	17.442
	4.50	0.0321	1.087	3.619	4.778	18.440
	4.75	0.0506	1.062	3.127	4.514	18.423
	5.00	0.0677	1.040	2.300	3.867	17.901
	5.25	0.0833	1.019	1.385	3.037	17.062
	5.50	0.0975	1.000	0.612	2.165	16.036
	5.75	0.1104	0.983	0.154	1.362	14.895
	6.00	0.1222	0.967	0.011	0.714	13.649
	6.50	0.1425	0.938	0.	0.077	11.010
7.00	0.1591	0.914	0.	0.000	8.326	

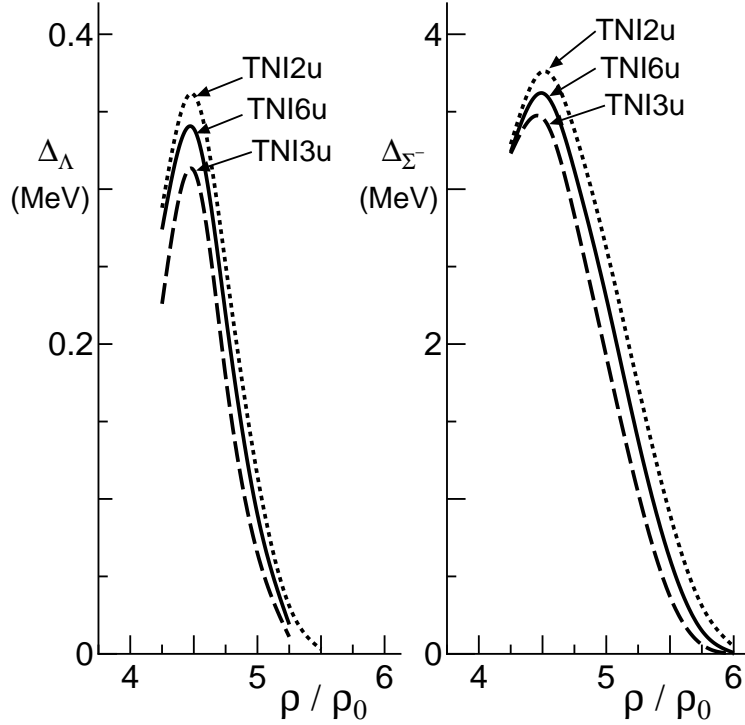


Fig. 7. Hyperon energy gap  $\Delta_Y$  for the ND-Soft pairing potential as a function of  $\rho$  for TNI2u, TNI6u and TNI3u EOSs. This reveals the strength of the EOS dependence of  $\Delta_Y$ . The left-hand (right-hand) side depicts the  $\Lambda(\Sigma^-)$  case.

(i) Both  $\Lambda$ - and  $\Sigma^-$ -superfluids are likely to exist in NS cores, since  $T_{c\Lambda}$  and  $T_{c\Sigma^-}$  are well above  $T_{in}$ .  $\Lambda$  and  $\Sigma^-$  become superfluids as soon as they appear in NS cores, and  $\Lambda$ -superfluidity is realized in a limited density region ( $\rho \sim (4 - 6)\rho_0$ ), while  $\Sigma^-$ -superfluid extends to much higher densities.

(ii) The behavior of the  $T_{cY}$  versus  $\rho$  relationships for three different potentials are more closely bunched in the  $\Lambda$  case than in the  $\Sigma^-$  case, which comes from the fact that there is less uncertainty in the pairing interaction in the  $\Lambda$  case, due to the experimental information from double  $\Lambda$  hypernuclei mentioned in §3.

(iii)  $T_{c\Sigma^-}$  ( $\sim 10^{10-11}$  K) for  $\Sigma^-$ -superfluid is larger than  $T_{c\Lambda}$  ( $\sim 10^9-10$  K) for  $\Lambda$ -superfluid by more than one order of magnitude, which comes mainly from the very large  $m_{\Sigma^-}^*$  ( $\sim 1$ ) compared to  $m_{\Lambda}^*$  ( $\sim 0.8$ ). The large  $T_{c\Sigma^-}$  implies that  $\Sigma^-$ -superfluidity can be realized in NSs even at an early stage of the thermal evolution, when  $T_{in}$  is as high as  $10^{10}$  K.

The full results for the hyperon energy gaps for TNI6u NS models and for three  $V_{YY}(^1S_0)$  are presented in Table III at several densities, together with the  $\rho$ -dependent input parameters,  $y_Y$  and  $m_Y^*$ , controlling the solution of the energy gap equations (3.1) – (3.4). In the cases of TNI3u and TNI2u, the points (i) – (iii) noted above are very similar to those in the TNI6u case. Thus, we can conclude

that  $\Lambda$  and  $\Sigma^-$  admixed in NS cores are certainly in the superfluid state, although this depends somewhat on the NS model and considerably on the pairing interaction  $V_{YY}(^1S_0)$ . The EOS-dependence of hyperon gap is shown in Fig.7.

#### 4.2. Effects of finite temperature

So far we have investigated the energy gaps at zero temperature. In cooling calculations of NSs, however, we need to take account of the temperature effects on the energy gaps, as the temperature  $T$  of  $Y$ -mixed NS matter varies during the thermal evolution and in general the resulting energy gap  $\Delta_Y$  decreases with increasing  $T$ .<sup>48)</sup> The  $T$ -dependent energy gaps  $\Delta_Y(T)$ , the solution of the finite-temperature gap equations (3.1) – (3.4), are plotted in Fig.8 for a typical case with ND-Soft and TNI6u. We observe that  $\Delta_Y$  depends remarkably on  $T$ , especially for small  $\Delta_Y$ . In the cooling calculations, it is of practical use to have a profile function  $P(\tau)$  approximating the  $T$ -dependence of  $\Delta_Y$ . Following our previous work,<sup>49)</sup> we introduce  $P(\tau)$  as a function of the argument  $\tau$  defined by  $\tau = T/T_c$ :

$$P_Y(\tau) \equiv \Delta_Y(q_{FY}, T) / \Delta_Y(q_{FY}, T = 0), \quad (4.2)$$

$$= 1 - \sqrt{2\pi a_0 \tau} \exp[-1/(a_0 \tau)] (1 + \alpha_1 \tau + \alpha_2 \tau^2), \quad (0 \leq \tau \leq \tau_b) \quad (4.3)$$

$$= a_0 C_1 \sqrt{1 - \tau} [1 + \beta_1 (1 - \tau) + \beta_2 (1 - \tau)^2], \quad (\tau_b \leq \tau \leq 1) \quad (4.4)$$

$$a_0 = a_0^* (T_c / T_c^*), \quad (4.5)$$

where  $a_0$ ,  $C_1$ ,  $\alpha_1$ ,  $\alpha_2$ ,  $\beta_1$  and  $\beta_2$  are constant parameters and  $a_0^* = 0.57$  is given by the coefficient appearing in the definition of  $T_c^*$  in Eq.(4.1). Here  $T_c$  ( $T_c^*$ ) denotes the actual (approximate) critical temperature. Equation (4.3) ensures that the energy gap ratio (Eq.(4.2)) decreases from  $P(\tau) = 1$  as  $T$  starts from  $T = 0$ , and Eq.(4.4) ensures that  $P(\tau) = 0$  at  $T = T_c$ .

From numerical calculations used to search for  $T_c$ , it is found that  $T_c$  is well substituted by  $T_c^*$ , except in the case of  $\Sigma^-$  with the FG-A potential, where, due to the particularly large  $\Delta_{\Sigma^-}$ , we have  $T_c \simeq (0.278 + 0.130(\rho/\rho_0)) \times T_c^*$  at densities  $(4 - 6)\rho_0$ . By selecting the boundary value of the two regions of  $\tau_b$  as  $\tau_b = 0.7$  and fitting  $\Delta(q_{FY}, T = 0)P(\tau)$  to  $\Delta(q_{FY}, T)$  actually calculated, we obtain the parameters of  $P(\tau)$  listed in Table IV (details of the procedure are given in Ref. 49)). The reproduction of  $\Delta(q_{FY}, T)/\Delta(q_{FY}, T = 0)$  by  $P(\tau)$  is illustrated in Fig.9 for  $\Lambda$  as an example. Once  $P(\tau)$  is obtained, we can use an analytic form of the  $T$ -dependent energy gap in NS cooling calculations by utilizing the zero temperature gap  $\Delta_Y(q_{FY}, T = 0)$ .

Table IV. Parameters for the profile function  $P(\tau) (\equiv \Delta_Y(T)/\Delta_Y(0))$  analytically representing the temperature dependence of the hyperon(Y) energy gap.

Y	$C_1$	$\alpha_1$	$\alpha_2$	$\beta_1$	$\beta_2$
$\Lambda$	2.8963	-0.45902	1.41171	-0.13926	-0.53396
$\Sigma^-$	2.8504	-0.39488	1.38328	-0.09447	-0.57033

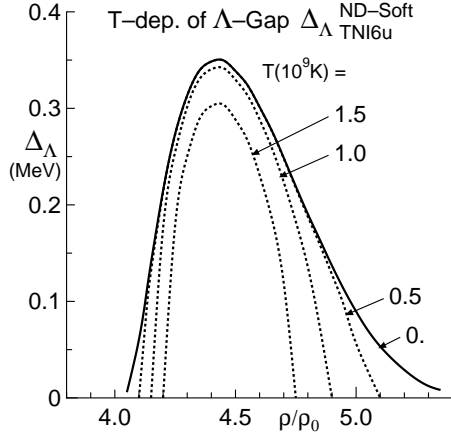


Fig. 8. Temperature ( $T$ ) dependence of the  $\Lambda$  energy gap ( $\Delta_\Lambda$ ) for the case of the TNI6u EOS and the ND-Soft potential, as an example.

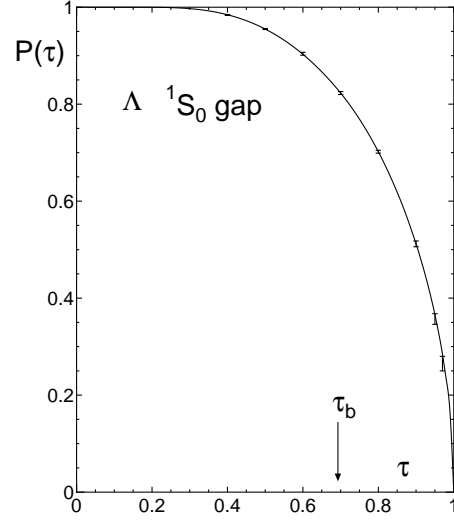


Fig. 9. Profile function  $P_\Lambda(\tau)$  ( $\equiv \Delta_\Lambda(T)/\Delta_\Lambda(0)$ ) in the form of Eqs.(4.3) and (4.4) as a function of  $\tau$  ( $\equiv T/T_{c\Lambda}$ ), averaged over the pairing potentials employed and the densities under consideration ( $\rho \simeq (4-5)\rho_0$ ). The crosses and the error bars denote the values obtained from numerical calculations of the finite-temperature gap equation. Here,  $\tau_b = 0.7$  denotes the boundary between the region of Eq.(4.3) and that of Eq.(4.4). The parameters for  $P_Y(\tau)$  ( $Y = \Lambda$  and  $\Sigma^-$ ) are listed in Table IV.

#### 4.3. Momentum triangle condition for $Y$ -DURca cooling

The  $\nu$ -emission process responsible for NS cooling acts only when a certain condition, namely, the so-called ‘‘momentum triangle condition’’ relevant to momentum conservation in the corresponding reaction, is satisfied. For example, a familiar  $\beta$ -decay process associated with nucleons ( $N$ ) and its inverse process (called  $N$ -DURca), i.e.,  $p \rightarrow n + l + \bar{\nu}_l$ ,  $n + l \rightarrow p + \nu_l$  (abbreviated as  $p \leftrightarrow nl$  hereafter), is allowed when the Fermi momenta  $k_i = q_{Fi} (= (3\pi^2 y_i \rho)^{1/3})$  for particles participating in the reaction satisfy the triangle condition

$$|k_p - k_l| < k_n < k_p + k_l. \quad (4.6)$$

Here the Fermi momentum  $k_\nu$  ( $\simeq \kappa_B T / \hbar c$ ) for neutrinos is omitted, because it is much smaller than those of  $N$  and  $l$ . As is well known,  $N$ -DURca is forbidden in usual neutron star matter including  $n$ ,  $p$ ,  $e^-$  and  $\mu^-$  components, because the second inequality in Eq.(4.6) is hard to hold among  $n$  (large component,  $y_n \gtrsim 0.9$ ),  $p$  (small component,  $y_p \lesssim 0.1$ ) and  $l$  (small component,  $y_l \lesssim 0.1$ ). Then, to satisfy the condition, it is necessary for another particle to participate as a bystander mediating momentum conservation. Indeed,  $\nu$ -emission due to the modified Urca

process ( $pN \leftrightarrow nNl$ ) including a bystander nucleon becomes a main agency for the cooling of usual NSs, although the  $\nu$ -emissivity is much smaller than that of the  $N$ -DUrca. In the case of normal NS matter ( $npe^- \mu^-$  matter), the fast cooling due to  $N$ -DUrca is made possible only for NS models including high proton fraction phase with  $y_p > 0.148$ .<sup>50)</sup>

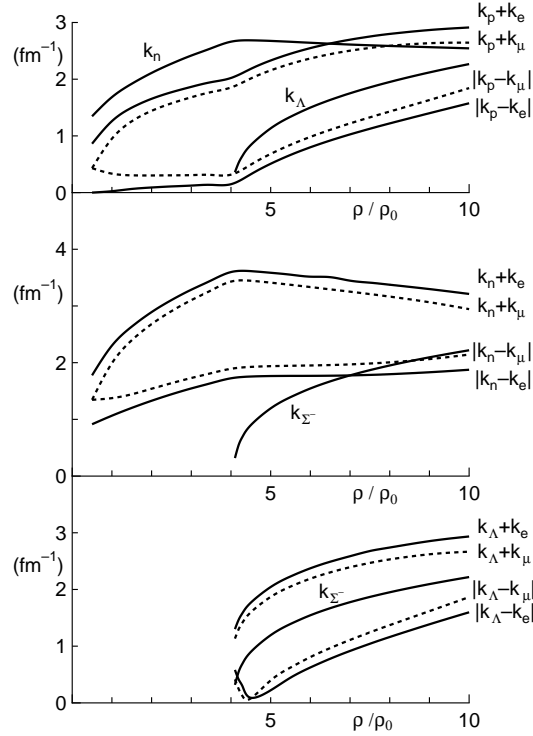


Fig. 10. Momentum triangle condition to check the functioning of various DUrca  $\nu$ -emission processes discussed in the text, where  $k_i = q_{Fi} = (3\pi^2 y_i \rho)^{1/3}$  is the Fermi momentum of the respective constituents ( $i = n, p, \Lambda, e^-, \mu^-$ ) in  $Y$ -mixed NS matter with TNI6u EOS; the upper panel depicts the  $n \leftrightarrow p + l$  process, the middle panel the  $\Sigma^- \leftrightarrow n + l$  process, and the lower panel the  $\Sigma^- \leftrightarrow \Lambda + l$  process, depending on  $\rho$ . The solid (dotted) lines corresponds to the case with  $l = e^-$  ( $\mu^-$ ).

How about the situation in the  $Y$ -mixed NS matter ( $np\Lambda\Sigma^-e^-\mu^-$  matter) under consideration? In Fig.10, the triangle condition is checked for DUrca processes, i.e.,  $N$ -DUrca and  $Y$ -DUrca, for the  $Y$ -mixed NS matter of TNI6u EOS by using the fractions  $y_i$  listed in Table II(b). The behavior for other EOS, the TNI2u EOS (Table II(a)) and TNI3u EOS (Table II(c)), are very similar to those in Fig.10. We note the following points:

- (i) In the  $Y$ -mixed phase, the proton fraction  $y_p$  becomes remarkably larger than that of usual NS matter ( $npe^- \mu^-$  matter), increasing with  $\rho$  and reaching 20% at  $\rho \sim 8\rho_0$ . However, Fig.10 shows that  $N$ -DUrca does not function up to the high density region, i.e.,  $\rho \lesssim 6.5\rho_0$  for  $n \leftrightarrow pe^-$  and  $\rho \lesssim 8\rho_0$  for  $n \leftrightarrow p\mu^-$ . Combining this with the  $M$ - $\rho_c$  relationship in Fig.2, this means that  $N$ -DUrca cooling begins



to function only for rather massive NSs with  $M \gtrsim 1.6M_\odot$  for  $n \leftrightarrow pe^-$  DUrca and  $M \gtrsim 1.7M_\odot$  for  $n \leftrightarrow p\mu^-$  DUrca.

(ii) In contrast with the  $N$ -DUrca mentioned above, the  $Y$ -DUrca of  $\Lambda \leftrightarrow pl$  type can operate as soon as  $\Lambda$  begins to appear, i.e., for  $\rho \gtrsim 4\rho_0$  both for  $l \equiv e^-$  and  $l \equiv \mu^-$ . This is because the triangle condition can be satisfied readily due to the fact that all the particles participating in the reactions belong to small components, not including the large  $n$ -component. From Fig.2, we see that  $\Lambda \leftrightarrow pl$   $Y$ -DUrca can work in all the  $Y$ -mixed NSs with  $M \gtrsim 1.35M_\odot$ , and it provides a very fast cooling of NSs.

(iii) It is difficult to realize conditions under which the  $Y$ -DUrca of  $\Sigma^- \leftrightarrow nl$  type including the large  $n$ -component functions. In fact, this is impossible for NSs with central density  $\rho_c \lesssim 7\rho_0$  for  $\Sigma^- \leftrightarrow ne^-$  and  $\rho_c \lesssim 8.5\rho_0$  for  $\Sigma^- \leftrightarrow n\mu^-$ . This implies that  $\Sigma^- \leftrightarrow nl$   $Y$ -DUrca occurs only for NS with  $M > 1.6M_\odot$  in the  $l \equiv e^-$  case and  $M > 1.7M_\odot$  in the  $l \equiv \mu^-$ . On the other hand, like the  $\Lambda \leftrightarrow pl$  type, the  $Y$ -DUrca of the  $\Sigma^- \leftrightarrow \Lambda l$  type occurs as soon as  $\Sigma^-$  appears, because all the associated particles are small components. It should be noted, however, that the  $Y$ -DUrca including  $\Sigma^-$  is made possible only for the density region where  $\Lambda$  coexists with  $\Sigma^-$ . That is, the participation of  $\Lambda$  in NS constituents is essential for the  $Y$ -DUrca to function.

Based on (i) – (iii), it is remarked that the momentum triangle condition interestingly limits the density region (in other words, NS mass) and the type of DUrca processes. Except in the case of massive NS stars,  $\Lambda$  mixing is a main mechanism for  $Y$ -DUrca cooling.

#### 4.4. Superfluid suppression effects on neutrino-emissivities

As mentioned in §1, the fast cooling due to  $Y$ -DUrca alone is not sufficient to explain colder class NSs, because its extremely efficient  $\nu$ -emission causes the serious problem of too rapid cooling. Here we discuss the suppression effects on  $\nu$ -emissivities due to nucleon and hyperon superfluidities, using the energy gaps in Table II and their  $T$ -dependence given by the profile function  $P(\tau)$  in §4.2. The  $Y$ -DUrca  $\nu$ -emissivities,  $\epsilon_{\text{DU}}(\Lambda \leftrightarrow p) \equiv \epsilon_{\text{DU}}(\Lambda \leftrightarrow pe^-) + (\Lambda \leftrightarrow p\mu^-)$  and  $\epsilon_{\text{DU}}(\Sigma^- \leftrightarrow \Lambda) \equiv \epsilon_{\text{DU}}(\Sigma^- \leftrightarrow \Lambda e^-) + \epsilon_{\text{DU}}(\Sigma^- \leftrightarrow \Lambda\mu^-)$ , are given by<sup>49)</sup>

$$\begin{aligned} \epsilon_{\text{DU}}(\Lambda \leftrightarrow p) &= 0.158 \times 10^{21} T_8^6 (y_e \rho / \rho_0)^{1/3} \\ &\quad \times m_\Lambda^* m_p^* (M_\Lambda M_p / M_n^2) R_{AA}(\Lambda, p) (\theta_e + \theta_\mu), \end{aligned} \quad (4.7)$$

$$\begin{aligned} \epsilon_{\text{DU}}(\Sigma^- \leftrightarrow \Lambda) &= 0.822 \times 10^{21} T_8^6 (y_e \rho / \rho_0)^{1/3} \\ &\quad \times m_{\Sigma^-}^* m_\Lambda^* (M_{\Sigma^-} M_\Lambda / M_n^2) R_{AA}(\Sigma^-, \Lambda) (\theta_e + \theta_\mu), \end{aligned} \quad (4.8)$$

where  $T_8 \equiv T/10^8$  K,  $\theta_l = 1$  (0) for the process allowed (not allowed) and  $R_{AA}(B_1, B_2)$  is the superfluid suppression factor relevant to the participating baryons  $B_1$  and  $B_2$ . The appearance of  $y_e$  comes from the chemical equilibrium;  $\mu_e = \mu_\mu \simeq \hbar q_{Fe} c$ . The quantity  $R_{AA}(B_1, B_2)$  is defined by the ratio of the integral of the statistical factors in the  $^1S_0$  superfluid phase ( $I_s$ ) to that in the normal phase ( $I_0$ ), i.e.,  $R_{AA}(B_1, B_2) \equiv I_s/I_0$ , which represents the decrease of the number density around the Fermi

surface due to the energy gap (further details including calculational methods are given in Ref. 49)).

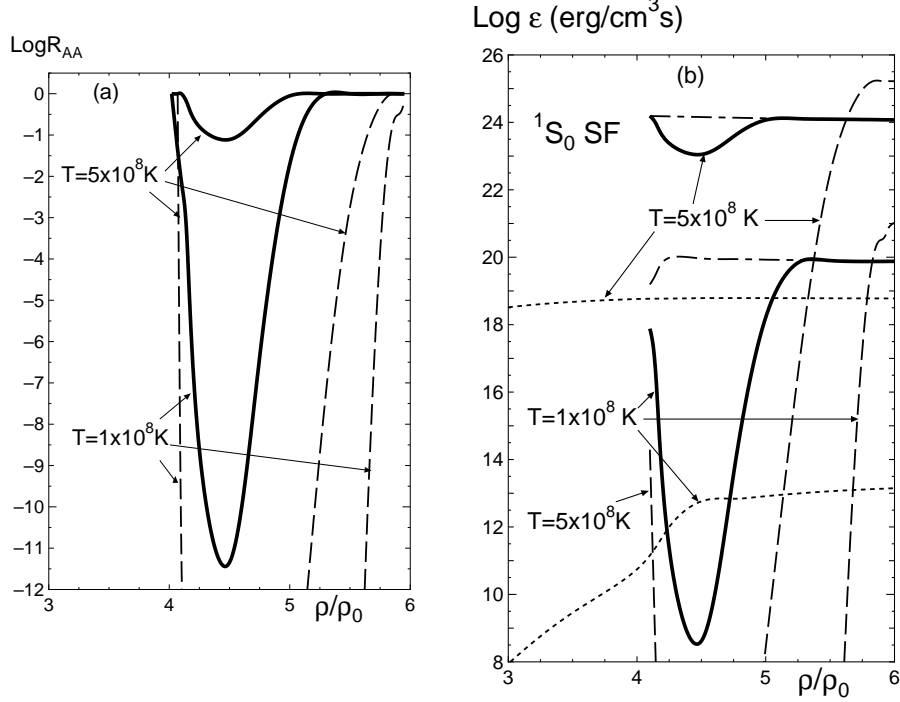


Fig. 11. (a) Superfluid suppression factor  $R_{AA}(B_1, B_2)$  for  $\nu$ -emissivity relevant to the baryons ( $B_1, B_2$ ) participating in the Y-DUrca processes, as functions of  $\rho$  and for two typical temperatures of the NS interior,  $T = 1 \times 10^8 \text{ K}$  and  $5 \times 10^8 \text{ K}$ . The solid lines (dashed lines) is for  $\Lambda \leftrightarrow p$ . ( $\Sigma^- \leftrightarrow \Lambda$ ) process summed over  $\Lambda \leftrightarrow p + e^-$  and  $\Lambda \leftrightarrow p + \mu^-$  ( $\Sigma^- \leftrightarrow \Lambda + e^-$  and  $\Sigma^- \leftrightarrow \Lambda + \mu^-$ ). (b) Y-DUrca  $\nu$ -emissivity including the superfluid suppression effect corresponding to  $R_{AA}(B_1, B_2)$  in (a), as functions of  $\rho$  and two typical temperatures. The solid lines (dashed lines) is for Y-DUrca of  $\Lambda \leftrightarrow p$  ( $\Sigma^- \leftrightarrow \Lambda$ ) type and the dotted lines are for the modified Urca processes responsible for the standard cooling of NSs. The emissivities without the superfluid suppression are also included as a reference and are plotted by the dash-dotted lines in the case of the  $\Lambda \leftrightarrow p$  process. Calculations in (a) and (b) are performed for TNI6u EOS and energy gaps from the ND-Soft pairing potential.

Calculated results are shown in Fig. 11 for TNI6u EOS and energy gaps from the ND-Soft pairing potential. Figure 11(a) demonstrates the suppression effects  $R_{AA}(B_1, B_2)$  as a function of  $\rho$  by considering two typical NS temperatures,  $T = 1 \times 10^8 \text{ K}$  and  $5 \times 10^8 \text{ K}$ .  $R_{AA}(B_1, B_2)$  depends strongly on both  $\rho$  and  $T$ , as reflected by the  $\rho$ - and  $T$ -dependent energy gaps of  $B_1$  and  $B_2$ . For example,  $R_{AA}(\Lambda, p)$  for  $\Lambda \leftrightarrow p$  process (solid lines) depends on  $\rho$  as  $R_{AA} \simeq 1 \rightarrow 10^{-1} \rightarrow 1$  for  $\rho/\rho_0 \simeq 4 \rightarrow 4.5 \rightarrow 5.0$  at  $T = 5 \times 10^8 \text{ K}$ . When the temperature decreases to  $T = 1 \times 10^8 \text{ K}$ , the suppression is much stronger;  $R_{AA} \simeq 1 \rightarrow 10^{-11.5} \rightarrow 1$ . Apart from the details, this characteristic feature can be qualitatively understood as resulting from an exponential damping factor,  $\exp[-(\Delta_{B_1} + \Delta_{B_2})/\kappa_B T]$  involved in  $R_{AA}(B_1, B_2)$ , together with the  $\rho$ - and  $T$ -dependences of  $\Delta_{B_1}$  and  $\Delta_{B_2}$  in Fig. 6 (in  $\Lambda \leftrightarrow p$  process,

$\Delta_p = 0$  as mentioned in §4.1.). For the  $\Sigma^- \leftrightarrow \Lambda$  process, the  $\rho$ - and  $T$ -dependent behavior of  $R_{AA}(\Sigma^-, \Lambda)$  is extremely enlarged because of the large energy gaps of  $\Sigma^-$ .

Figure 11(b) illustrates how the emissivities  $\epsilon_{\text{DU}}(B_1 \leftrightarrow B_2)$  for  $Y$ -DUrca are moderated by  $R_{AA}(B_1, B_2)$ , where the emissivities  $\epsilon_{\text{MD}}$  for the modified Urca including superfluid suppression (see Ref. 49) for details) are also shown for comparison. First, we consider  $\epsilon(\Lambda \leftrightarrow p)$  (solid lines) in the density range  $\rho \simeq (4-5)\rho_0$ . At  $T = 5 \times 10^8$  K, the effect of  $R_{AA}(\Lambda, p)$  is not significant and  $\epsilon_{\text{DU}}(\Lambda \leftrightarrow p) \sim 10^{23-24}$  erg/cm<sup>3</sup>s is much larger than  $\epsilon_{\text{MU}} \sim 10^{18-19}$  erg/cm<sup>3</sup>s. However, at  $T = 1 \times 10^8$  K, the situation is very different;  $\epsilon_{\text{DU}}(\Lambda \leftrightarrow p) \sim 10^{20}$  erg/cm<sup>3</sup>s for no suppression (dash-dotted lines) is maximumly suppressed to  $\epsilon_{\text{DU}}(\Lambda \leftrightarrow p) \sim 10^{8.5}$  erg/cm<sup>3</sup>s by  $R_{AA}(\Lambda, p)$  and is even smaller than  $\epsilon_{\text{MU}} \sim 10^{12-13}$  erg/cm<sup>3</sup>s for  $\rho \sim (4.2-4.7)\rho_0$ , although  $\epsilon_{\text{DU}}(\Lambda \leftrightarrow p) \gtrsim \epsilon_{\text{MU}}$  continues to hold for other densities. The behavior of  $\epsilon_{\text{DU}}(\Lambda \leftrightarrow p)$  for  $T = 5 \times 10^8$  K  $\rightarrow 1 \times 10^8$  K reveals that at higher  $T$  in relatively earlier stage of the thermal evolution, the  $\Lambda \leftrightarrow p$  process dramatically accelerates the NS cooling as compared to the standard modified Urca process, but this acceleration experiences a braking effect due to superfluid suppression as  $T$  decreases in later stage, and in this way, too rapid cooling does not occur. In the case of the  $\Sigma^- \leftrightarrow \Lambda$  process,  $\epsilon_{\text{DU}}(\Sigma^- \leftrightarrow \Lambda)$  is much smaller than  $\epsilon_{\text{MU}}$ , as well as  $\epsilon_{\text{DU}}(\Lambda \leftrightarrow p)$ , for  $\rho \sim (4-5)\rho_0$ , due to the extremely strong suppression caused by  $R_{AA}(\Sigma^-, \Lambda)$ . In the total  $\nu$ -emissivity, the most efficient  $\nu$ -emission process is of prime importance. So the  $\Sigma^- \leftrightarrow \Lambda$  process becomes appreciable only at high densities ( $\rho \gtrsim 5.5\rho_0$ ) where  $\epsilon_{\text{DU}}(\Sigma^- \leftrightarrow \Lambda)$  becomes comparable to or larger than  $\epsilon_{\text{DU}}(\Lambda \leftrightarrow p)$ , depending on  $T$ . At high densities ( $\rho > 5\rho_0$ ),  $\epsilon_{\text{DU}}(\Lambda \leftrightarrow p)$  and/or  $\epsilon_{\text{DU}}(\Sigma^- \leftrightarrow \Lambda)$  suffer no suppression, because of the disappearance of the superfluidities, and hence massive NSs with  $\rho_c > 5\rho_0$  cause a problem of too rapid cooling. This undesirable situation is the same as that for the  $N$ -DUrca cooling mentioned in §4.1 which becomes possible for  $\rho \gtrsim 6.5\rho_0$ , because the  $n$  and  $p$  superfluidities completely disappear for such high densities.

Taking notice of the two conditions, i.e., the triangle condition to allow fast DUrca cooling and the superfluid suppression condition to moderate the cooling rate (avoiding too rapid cooling), we can say that the  $Y$ -DUrca of  $\Lambda \leftrightarrow p$  type plays a decisive role in bringing about the cooling scenario for colder class NSs.<sup>49)</sup> This is because firstly the  $\Sigma^- \leftrightarrow \Lambda$  process can function only with the coexistence of  $\Lambda$  and secondly the large  $\Sigma^-$  gap suppresses  $\epsilon_{\text{DU}}(\Sigma^- \leftrightarrow \Lambda)$  too strongly. To obtain consistency with surface temperature observations of NSs, we can constrain the mass of the colder class NSs as follows. For the TNI6u NS models, it must be larger than about  $1.35M_\odot$  in order to realize  $\rho_c > \rho_t(Y)$  and also be smaller than about  $1.55M_\odot$  in order to avoid too rapid cooling. Of course this mass restriction depends on the NS model (Fig.2) and the superfluid gap  $\Delta$  (Fig.6), but in any case the functioning of the  $Y$ -DUrca moderated by the baryon superfluidity provides us with a new idea regarding NS cooling. That is, less massive NSs (hence without  $Y$ -mixed core) cooled slowly by the standard process (modified Urca) correspond to hotter class NSs, and massive NSs (with  $Y$ -mixed core and superfluids) cooled rapidly by the nonstandard process ( $Y$ -DUrca) correspond to colder class NSs. In

fact, cooling calculations (although of a preliminary nature), nicely account for the surface temperature observations employing this idea.<sup>10)</sup>

### §5. Less attractive $\Lambda\Lambda$ interaction

We have discussed that the hyperon cooling scenario for NSs is consistent with observations and the occurrence of  $\Lambda$ -superfluidity is of particular importance. There exists, however, an experimental result that is incompatible with this occurrence. Recently the KEK-E373 group observed one event of the  $\Lambda$  hypernucleus  ${}^6_{\Lambda\Lambda}\text{He}$  in an emulsion experiment, called the ‘‘NAGARA event’’ and extracted new information of  $\Delta B_{\Lambda\Lambda} \simeq 1$  MeV for the  $\Lambda\Lambda$  bond energy from the difference between the binding energies  $B$  of double and single  $\Lambda$  hypernuclei:<sup>46)</sup>

$$\Delta B_{\Lambda\Lambda} = B({}^6_{\Lambda\Lambda}\text{He}) - 2 \times B({}^5_{\Lambda}\text{He}). \quad (5.1)$$

The new result  $\Delta B_{\Lambda\Lambda} \simeq 1$  MeV is much smaller than the old one  $\Delta B_{\Lambda\Lambda} \simeq (4 - 5)$  MeV extracted from  ${}^{10}_{\Lambda\Lambda}\text{Be}$  and  ${}^{13}_{\Lambda\Lambda}\text{B}$ . This suggests that the  $\Lambda\Lambda$  attraction responsible for  $\Lambda$ -superfluidity would be much weaker than previously thought. Since all the pairing interactions, ND-Soft, Ehime and FG-A, used in the present calculations of the  $\Lambda$ -gap (§3) are taken to be consistent with the old  $\Delta B_{\Lambda\Lambda} \simeq (4 - 5)$  MeV, the new finding of  $\Delta B_{\Lambda\Lambda} \simeq 1$  MeV must be considered seriously and it necessitates a reexamination of  $\Lambda$ -gaps for the reduced  $\Lambda\Lambda$  attraction. Hiyama et al.,<sup>51)</sup> performing energy calculations for the  $\alpha + \Lambda + \Lambda$  system, found that  $\Delta B_{\Lambda\Lambda} \simeq 1$  MeV is reproduced by taking  $V_{\Lambda\Lambda}^{\text{ND}}({}^1S_0) \rightarrow \tilde{V}_{\Lambda\Lambda}^{\text{ND}}({}^1S_0) \simeq 0.5V_{\Lambda\Lambda}^{\text{ND}}({}^1S_0)$ . More precisely, the potential strength in the modified ND-Soft  $\tilde{V}_{\Lambda\Lambda}^{\text{ND}}({}^1S_0)$  is multiplied by a factor of 0.45 for the shortest-range term and a factor of 0.5 for the intermediate- and long-range terms. By using this  $\tilde{V}_{\Lambda\Lambda}^{\text{ND}}({}^1S_0)$ , we have tried to calculate  $\Delta_\Lambda$  and found that  $\Lambda$ -superfluidity does not occur, i.e.,  $T_c(\Lambda) \ll T_{in} \simeq 10^8$  K. This leads us to inquire about the situation for  $\Delta_{\Sigma^-}$  since  $YY$  interactions are internally related according to the OBE plus  $SU(3)$  symmetry hypothesis. To see this, we reconstruct the  $BB$  interaction model of FG-A so as to reproduce the  $\Lambda\Lambda$  phase shifts from  $\tilde{V}_{\Lambda\Lambda}^{\text{ND}}({}^1S_0)$  by weakening the attractive contribution from the  $\sigma$ -meson exchange. Through new parameters adjusted, new  $\Sigma^- \Sigma^-$  interaction  $\tilde{V}_{\Sigma^- \Sigma^-}^{\text{FG}}$  is to be obtained. This can be done as follows.<sup>52)</sup>

In the framework of octet baryons plus nonet mesons with  $SU(3)$  symmetry, the coupling constants  $\tilde{g}_{BBm} = g_{BBm}/\sqrt{4\pi}$  for the  $BB$  interaction by single meson ( $m$ ) exchange are given in terms of four parameters, i.e., the singlet coupling  $\tilde{g}^{(1)}$ , the octet coupling  $\tilde{g}^{(8)}$ , a parameter  $\alpha$  relevant to the so-called F-D ratio, and the mixing angle  $\theta$ . Therefore, the set of these four parameters is uniquely determined when four coupling constants are given. Here we stipulate that the  $NN$  interaction sector be unaltered as it is firmly established. There we use, as four coupling constants,  $\tilde{g}_{NN\sigma}$ ,  $\tilde{g}_{NNa_0}$  and  $\tilde{g}_{NNf_0}$  which are unchanged from the original FG-A model, and  $\tilde{g}_{\Lambda\Lambda\sigma}$  which is adjusted so as to reproduce the phase shifts from  $\tilde{V}_{\Lambda\Lambda}^{\text{ND}}({}^1S_0)$  compatible

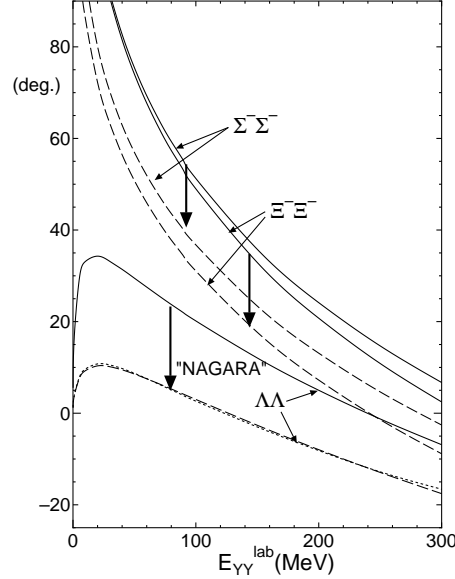


Fig. 12. A demonstration of to show how the attractive features of  $^1S_0$   $YY$  interactions (Fig.4) are weakened by taking account of the less attractive  $\Lambda\Lambda$  interaction suggested by the “NAGARA event”  $^6_{\Lambda\Lambda}\text{He}$  in the framework of OBE plus  $SU(3)$  symmetry. The solid lines (dashed lines) are the  $^1S_0$  phase shifts for the original FG-A potential  $V_{YY}^{\text{FG}}$  (the modified FG-A potential  $\tilde{V}_{YY}^{\text{FG}}$ ). The modification ( $V_{YY}^{\text{FG}} \rightarrow \tilde{V}_{YY}^{\text{FG}}$ ) has been done through the fitting of  $\tilde{V}_{\Lambda\Lambda}^{\text{FG}}$  to  $\tilde{V}_{\Lambda\Lambda}^{\text{ND}}$  obtained by seeking reproduction of the  $\Lambda\Lambda$  bond energy of  $^6_{\Lambda\Lambda}\text{He}$ . The phase shifts from  $\tilde{V}_{\Lambda\Lambda}^{\text{ND}}$  are shown by the dotted line for reference.

with the experimental results for  $^6_{\Lambda\Lambda}\text{He}$ :

$$\tilde{g}_{NN\sigma} = \tilde{g}^{(1)} \cos \theta + (4\alpha - 1)/\sqrt{3} \cdot \tilde{g}^{(8)} \sin \theta, \quad (5.2a)$$

$$\tilde{g}_{NNa_0} = \tilde{g}^{(8)} \quad (5.2b)$$

$$\tilde{g}_{NNf_0} = (4\alpha - 1)/\sqrt{3} \cdot \tilde{g}^{(8)} \cos \theta - \tilde{g}^{(1)} \sin \theta, \quad (5.2c)$$

$$\tilde{g}_{\Lambda\Lambda\sigma} = \tilde{g}^{(1)} \cos \theta - 2(1 - \alpha)/\sqrt{3} \cdot \tilde{g}^{(8)} \sin \theta. \quad (5.2d)$$

Actually, about 10% reduction of  $\tilde{g}_{\Lambda\Lambda\sigma}$  is satisfactory for the reproduction of the phase shifts at low scattering energies ( $\lesssim 50$  MeV) corresponding to the pairing problem of  $\Lambda$ . From the new set  $\{\tilde{g}^{(1)}, \tilde{g}^{(8)}, \alpha, \theta\}$ , new  $\tilde{g}_{\Lambda\Lambda m}$  and  $\tilde{g}_{\Sigma^-\Sigma^- m}$  responsible for the modified  $\tilde{V}_{\Lambda\Lambda}^{\text{FG}}(^1S_0)$  and  $\tilde{V}_{\Sigma^-\Sigma^-}^{\text{FG}}(^1S_0)$  are obtained as in Table V. Figure 12 compares the attractive effects of  $V_{YY}^{\text{FG}}(^1S_0)$  (solid lines) and  $\tilde{V}_{YY}^{\text{FG}}(^1S_0)$  (dashed lines) in terms of their phase shifts. We see that the  $\Sigma^-\Sigma^-$  attraction of modified FG-A, as in the  $\Lambda\Lambda$  case, is significantly reduced from that of the original FG-A. However,  $\tilde{V}_{\Sigma^-\Sigma^-}^{\text{FG}}(^1S_0)$  remains to be more attractive than the original  $V_{\Lambda\Lambda}^{\text{ND}}(^1S_0)$ , implying the persistence of  $\Sigma^-$ -superfluidity. In fact, a reexamination of  $\Delta_{\Sigma^-}$  with  $\tilde{V}_{\Sigma^-\Sigma^-}^{\text{FG}}(^1S_0)$  shows that  $\Sigma^-$ -superfluidity is realized with  $T_c(\Sigma^-)$  reduced by about a half, as indicated by an arrow in Fig.6. Also note that Fig.12 shows that the situation for the  $\Xi^-\Xi^-$  case is similar to the  $\Sigma^-\Sigma^-$  case, suggesting that  $\Xi^-$  when admixed in

NS cores could be in a superfluid state.

To summarize, the less attractive  $\Lambda\Lambda$  interaction suggested by the NAGARA event leads to the disappearance of  $\Lambda$ -superfluid, although  $\Sigma^-$  superfluidity can persist, and the  $Y$ -cooling scenario encounters the serious problem of too rapid cooling because the superfluid suppression of the  $\nu$ -emissivity for the  $\Lambda \leftrightarrow pl$  process does not occur.

Table V. Coupling constant  $\tilde{g}_{YYm}$  for the modified FG-A potential ( $\tilde{V}_{YY}^{FG}$ ) to take account of “NAGARA event” data. The numbers in the parentheses are for original FG-A potential ( $V_{YY}^{FG}$ ).

$\tilde{g}_{YYm} \setminus m$	$\sigma$	$f_0$	$a_0$
$\tilde{g}_{\Lambda\Lambda m}$	4.656 (5.15543)	2.0849 (2.46243)	0 (0)
$\tilde{g}_{\Sigma^- \Sigma^- m}$	4.4265 (5.53592)	-2.5360 (-1.41267)	5.5307 (4.89611)
$\tilde{g}_{\Xi^- \Xi^- m}$	4.3610 (5.66490)	-3.8542 (-2.72596)	4.7687 (4.13408)

## §6. Summary and remarks

We have calculated the energy gaps of  $\Lambda$  and  $\Sigma^-$  admixed in NS cores for values of the mixing ratios and effective mass parameters of the  $Y$ -mixed NS models obtained realistically using  $G$ -matrix-based effective interaction approach, and by adopting several pairing potentials to take account of the uncertainties on the  $YY$  interactions. It is found that both  $\Lambda$ - and  $\Sigma^-$ -superfluids are realized as soon as they begin to appear at around  $4\rho_0$ , although the critical temperature and maximum density for the existence of the gaps depend considerably on the pairing potential. The EOSs for  $Y$ -mixed NS matter with different stiffnesses, together with the fractions of the respective components, and also the  $\Lambda$ - and  $\Sigma^-$ -energy gaps were numerically determined and tabulated. The profile function  $P(\tau)$  is presented to give analytically the temperature dependence of energy gaps. The presentation of these physical quantities serves as physical inputs for the calculations of  $Y$ -cooling for NSs.

Occurrence of  $Y$  superfluidity is indispensable to the  $Y$ -cooling scenario to be consistent with observations of colder class NSs, because otherwise enormous  $\nu$ -emissivities due to  $Y$ -DUrca processes cannot be moderated by superfluid suppression effects and this would cause a serious problem of too rapid cooling generally encountered in DUrca processes. The momentum triangle conditions to discriminate the functioning DUrca processes were checked in  $Y$ -mixed NS matter. By combining the effects of superfluid suppression, it was found that in the  $Y$ -DUrca processes only the  $\Lambda \leftrightarrow pl$  and  $\Sigma^- \leftrightarrow \Lambda l$  processes can function, and the former plays a decisive role in  $Y$ -cooling, whereas the latter is completely suppressed due to the large  $\Sigma^-$  gaps except in the particular dense core of NSs. The  $N$ -DUrca in its currently accepted form is excluded for the fast cooling scenario, because it does not take place in core densities of medium mass NSs and its functioning in massive NSs encounters the problem of too rapid cooling owing to the complete disappearance of nucleon energy gaps. On the basis of the investigations presented here, we conclude that there

is a strong possibility that the  $Y$ -cooling scenario combined with  $Y$ -superfluidity is a promising candidate for nonstandard fast cooling of NSs. This scenario can explain observations according to which the hotter class NSs have lighter masses (e.g.,  $M \lesssim 1.35M_\odot$  for TNI6u plus ND-Soft and no  $Y$ -mixed core) and are cooled slowly by the standard modified Urca, while colder class NSs have medium masses ( $M \sim (1.4-1.5)M_\odot$  with  $Y$ -superfluids) and are cooled rapidly by a moderated non-standard cooling of  $Y$ -DUrca. The massive NSs ( $M \gtrsim 1.55M_\odot$ ) including a dense core with the disappearance of  $Y$ -superfluids causes too rapid cooling and are excluded if extremely cooled NSs are not found. It is worth noting that observations of the surface temperature interestingly limit the mass of NSs.

The less attractive  $\Lambda\Lambda$  interaction inferred from the NAGARA event  ${}^6_{\Lambda\Lambda}\text{He}$  affects so much the  $Y$ -cooling scenario. It was shown that  $\Lambda$ -superfluidity disappears when this weaker attraction is taken into account although  $\Sigma^-$ -superfluidity survives. This leads to the consideration that the  $Y$ -cooling scenario, where  $\Lambda$ -superfluid plays an essential role, breaks down due to too rapid cooling. However, we cannot draw a final conclusion in this regard until the less attractive  $\Lambda\Lambda$  interaction not to allow  $\Lambda$ -superfluidity is confirmed by more extensive studies on the following issues: the validity of extracting the  $\Lambda\Lambda$  bond energy of a  ${}^6_{\Lambda\Lambda}\text{He}$  system using Eq.(5.1) without considering the rearrangement effects, the possibility of a small  $\Delta B_{\Lambda\Lambda}$  as a result of the three-body force repulsion, the mass-number dependence of  $\Delta B_{\Lambda\Lambda}$  in double  $\Lambda$  hypernuclei, possible effects of  $\Lambda\Lambda$ - $\Sigma\Sigma$ - $\Xi N$  channel coupling in the  $\Lambda\Lambda$  pairing,  $\Lambda$ -superfluidity due to  $\Lambda\Sigma^-$  pairing not restricted to  $\Lambda\Lambda$  pairing, and of course the new finding of double  $\Lambda$  hypernuclei. For example, it is of importance to note that the inclusion of rearrangement effects on the  $\alpha$ -particle in the  $\alpha + \Lambda + \Lambda$  system suggests a stronger  $\Lambda\Lambda$  attraction than  $\hat{V}_{\Lambda\Lambda}^{\text{ND}}({}^1S_0)$ .<sup>53),54)</sup>

Finally, it is worth while mentioning another possibility for the fast cooling scenario. As is well known, several processes of nonstandard fast cooling of the DUrca type have been proposed. These function under the possible presence of nonstandard components, such as a pion condensate ( pion cooling), kaon condensate (kaon cooling), high proton-fraction phase ( $N$ -DUrca cooling) and quark phase (quark cooling). Among these,  $N$ -DUrca and kaon coolings are excluded from the candidates for fast cooling scenario consistent with observations, because baryon superfluidity is unlikely in these exotic phases.<sup>55)</sup> Also quark cooling is excluded because of too large energy gaps exceeding several tens of MeV which completely suppress the  $\nu$ -emission. Then, only pion cooling remains as another promising candidate because there is a strong possibility of quasibaryon superfluids due mainly to the large effective masses and pairing attraction enhanced by isobar  $\Delta(1232)$  contamination.<sup>57),58)</sup>

### Acknowledgements

The authors wish to thank S. Tsuruta and T. Tatsumi for their cooperative discussion about the cooling problem of neutron stars and also M. Wada for his helpful discussion on the use of the Funabashi-Gifu baryon-baryon interaction model. We are grateful for the financial support provided by Grant-in-Aid for Scientific Research (C) from the Ministry of Education, Culture, Sports, Science and Technology

(16540225 and 15540244).

### References

- 1) T. Takatsuka, S. Nishizaki, Y. Yamamoto and R. Tamagaki, *Proc. 7th Int. Conf. on "Hypernuclear and Strange Particle Physics" (HYP2000), Torino, Italy, Oct.23-27, 2000*, ed.E. Botta, T. Bressami and A. Feliciello, Nucl. Phys. **A 691** (2001), 254C.
- 2) T. Takatsuka, S. Nishizaki, Y. Yamamoto and R. Tamagaki, *Prog. Theor. Phys. Suppl. No.146* (2002), 279.
- 3) T. Takatsuka, *Prog. Theor. Phys. Suppl. No.156* (2004), 84.
- 4) S. Tsuruta, *Comments Astrophys.* **11** (1986), 151.
- 5) S. Tsuruta, *Proc. US-Japan Joint Seminar on "The Structure and Evolution of Neutron Stars", Kyoto, Japan, 1990*, ed. D. Pines, R. Tamagaki and S. Tsuruta (Addison-Wesley, 1992), p371.
- 6) S. Tsuruta, *Phys. Rep.* **292** (1998), 1.
- 7) H. Umeda, S. Tsuruta and K. Nomoto, *Astrophys. J.* **433** (1994), 256.
- 8) H. Umeda, K. Nomoto, S. Tsuruta, T. Muto and T. Tatsumi, *Astrophys. J.* **431** (1994), 309.
- 9) S. Tsuruta, M.A. Teter, T. Takatsuka, T. Tatsumi and R. Tamagaki, *Astrophys. J.* **571** (2002), L143.
- 10) S. Tsuruta, *Proc. of the 218th IAU Symposium on "Young Neutron Stars and Their Environments", Sydney, Australia, July 2003*, ed. F. Camilo and B.M. Gaonsler, Vol.218 (2004), p.21.
- 11) C.J. Pethick, *Rev. Mod. Phys.* **64** (1992), 1133.
- 12) M. Prakash, *Phys. Rep.* **242** (1994), 297.
- 13) D. Page and E. Baron, *Astrophys. J.* **354** (1990), L17.
- 14) D. Page and J. Applegate, *Astrophys. J.* **394** (1992), L17.
- 15) Ch. Schaab, D. Voskresensky, A.D. Sedrakian, F. Weber and M.K. Weigel, *Astron. Astrophys.* **321** (1997), 591.
- 16) D.G. Yakovlev, A.D. Kaminker, O.Y. Gnedin and P. Haensel, *Phys. Rep.* **354** (2001), 1.
- 17) D.G. Yakovlev and C.J. Pethick, *Annu. Rev. Astron. Astrophys.* **42** (2004), 169.
- 18) D. Blaschke, H. Grigorian and D.N. Voskresensky, *Astron. Astrophys.* **424** (2004), 979.
- 19) Mad. Prakash, Man. Prakash, J.M. Lattimer and C.J. Pethick, *Astrophys. J.* **390** (1992), L77.
- 20) T. Takatsuka and R. Tamagaki, *Prog. Theor. Phys.* **102** (1999), 1043; *Proc. Int. Symposium on "Physics of Hadrons and Nuclei", Tokyo, Japan, Dec. 14-17, 1998*, ed. Y. Akaishi, O. Morimatsu, M. Oka and K. Shimizu, Nucl. Phys. **A 670** (2000), 222c; *Proc. APCTP Workshop on "Strangeness Nuclear Physics" (SNP'99), Seoul, Korea, Feb. 19-22,1999*, ed. I-T. Cheon, S-W. Hong and T. Motoba (World Scientific, 2000), p.337.
- 21) T. Takatsuka, S. Nishizaki, Y. Yamamoto and R. Tamagaki, *Proc. the 1st Asian-Pacific Conference on "Few-Body Problems in Physics '99", Tokyo, Japan, Aug.23-28, 1999*, ed. S. Oryu, M. Kamimura and S. Ishikawa, *Few Body Systems Suppl.* **12** (2000), p.108; *Proc. the 10th Int. Conf. "Recent Progress in Many-Body Theories", Seattle, USA, Sept. 10-15, 1999*, ed. R. F. Bishop, K. A. Gernoth, N. R. Walet and Y. Xian, *Advances in Quantum Many-Body Theory*, **3** (World Scientific, 2000), p.323; *Proc. Int. Symposium on "Origin of Matter and Evolution of Galaxies 2000", Tokyo, Japan, Jan. 19-21, 2000*, ed. T. Kajino, S. Kubono, K. Nomoto and I. Tanihata, (World Scientific, 2003), p.305.
- 22) T. Takatsuka, S. Nishizaki, Y. Yamamoto and R. Tamagaki, *Prog. Theor. Phys.* **105** (2001), 179.
- 23) S. Nishizaki, Y. Yamamoto and T. Takatsuka, *Prog. Theor. Phys.* **105** (2001), 607.
- 24) T. Takatsuka, S. Nishizaki and Y. Yamamoto, *Proc. the Int. Symposium on "Perspectives in Physics with Radioactive Isotope Beams 2000 (RIB00)", Hayama, Kanagawa, Japan, Nov. 13-16, 2000*, ed. K. Asahi, H. Sakai, I. Tanihata, T. Nakamura, C. Signorini and Th. Walcher, *Eur. Phys. J. A* **13** (2002), 213.
- 25) S. Nishizaki, Y. Yamamoto and T. Takatsuka, *Prog. Theor. Phys.* **108** (2002), 703.
- 26) M.M. Nagels, T.A. Rijken and J.T. deSwart, *Phys. Rev. D* **12** (1975), 744; *Phys. Rev. D* **15** (1977), 2547; *Phys. Rev. D* **20** (1979), 1633.
- 27) Y. Yamamoto, S. Nishizaki and T. Takatsuka, *Prog. Theor. Phys.* **103** (2000), 981.



- 28) S. Nishizaki, T. Takatsuka, N. Yahagi and J. Hiura, *Prog. Theor. Phys.* **86** (1991), 853.
- 29) S. Nishizaki, T. Takatsuka and J. Hiura, *Prog. Theor. Phys.* **92** (1994), 93.
- 30) I.E. Lagaris and V.R. Pandharipande, *Nucl. Phys.* **A 369** (1981), 470.
- 31) B. Friedman and V.R. Pandharipande, *Nucl. Phys.* **A 361** (1981), 502.
- 32) R.B. Wiringa, V. Fiks and A. Fabrocini, *Phys. Rev.* **C 38** (1988), 1010.
- 33) A. Akmal, V.R. Pandharipande and D.G. Ravenhall, *Phys. Rev.* **C 58** (1998), 1804.
- 34) M. Baldo, G.F. Burgio and H.-J. Schulze, *Phys. Rev.* **C 61** (2000), 055801.
- 35) I. Vidana, A. Ramos, L. Engvik and M. Hjorth-Jensen, *Phys. Rev.* **C 62** (2000), 035801.
- 36) T. Tanigawa, M. Matsuzaki and S. Chiba, *Phys. Rev.* **C 68** (2003), 015801.
- 37) S. Balberg and N. Barnea, *Phys. Rev.* **C 57** (1998), 409.
- 38) E. Hiyama, M. Kamimura, T. Motoba, T. Yamada and Y. Yamamoto, *Prog. Theor. Phys.* **97** (1997), 881.
- 39) T. Ueda, K. Tominaga, M. Yamaguchi, N. Kijima, D. Okamoto, K. Miyagawa and T. Yamada, *Prog. Theor. Phys.* **99** (1998), 891; *Nucl. Phys.* **A 642** (2000), 995.
- 40) I. Arisaka, K. Nakagawa, S. Shinmura and M. Wada, *Prog. Theor. Phys.* **104** (2000), 995.
- 41) M. Danyasz et al., *Nucl. Phys.* **49** (1963), 121.
- 42) S. Aoki et al., *Prog. Theor. Phys.* **85** (1991), 1287.
- 43) Y. Yamamoto, T. Motoba, H. Himeno, K. Ikeda and S. Nagata, *Prog. Theor. Phys. Suppl.* No.117 (1994), 361.
- 44) T. Yamada and C. Nakamoto, *Phys. Rev.* **C 62** (2000), 034319.
- 45) C.B. Dover, D.J. Millener, A. Gal and D.H. Davis, *Phys. Rev.* **C 44** (1991), 1905.
- 46) H. Takahashi et al., *Phys. Rev. Lett.* **87** (2001), 212502.
- 47) R. Tamagaki, *Prog. Theor. Phys.* **39** (1968), 91.
- 48) T. Takatsuka and R. Tamagaki, *Proc. the 16th Int. Conf. on "Particles and Nuclei (PANIC '02)", Osaka, Japan, Sep. 30-Oct. 4, 2002*, ed. H. Toki, K. Imai and T. Kishimoto, *Nucl. Phys.* **A 721** (2003), 1003c.
- 49) T. Takatsuka and R. Tamagaki, *Prog. Theor. Phys.* **112** (2004), 37; *Proc. Int. Conf. on "Clustering Aspects of Nuclear Structure and Dynamics"*, ed. K. Ikeda, I. Tanihata and H. Horiuchi, *Nucl. Phys.* **A 738** (2004), C387.
- 50) J.M. Lattimer, C.J. Pethick, M. Prakash and P. Haensel, *Phys. Rev. Lett.* **66** (1991), 2701.
- 51) E. Hiyama, M. Kamimura, T. Motoba, T. Yamada and Y. Yamamoto, *Phys. Rev.* **C 66** (2002), 024007.
- 52) R. Tamagaki and T. Takatsuka, *Soryushiron Kenkyu (Kyoto)* **106** (2002), B85.
- 53) H. Nemura, Y. Akaishi and Y. Suzuki, *Phys. Rev. Lett.* **89** (2002), 142504.
- 54) Q.N. Usmani, A.R. Bodmer and B. Sharma, *Phys. Rev.* **C 70** (2004), 061001.
- 55) T. Takatsuka and R. Tamagaki, *Prog. Theor. Phys.* **94** (1995), 457; *Prog. Theor. Phys.* **97** (1997), 345.
- 56) T. Takatsuka and R. Tamagaki, *Prog. Theor. Phys. Suppl.* No.112 (1993), 107.
- 57) T. Takatsuka and R. Tamagaki, *Prog. Theor. Phys.* **98** (1997), 393; *Prog. Theor. Phys.* **101** (1999), 1043.
- 58) R. Tamagaki and T. Takatsuka, *Prog. Theor. Phys.* **115**, No.1 (2006).